J. Fluid Mech. (2006), *vol.* 550, *pp.* 307–347.
doi:10.1017/S0022112005008220 Printed in the United Kingdom

Acoustic radiation of Tollmien–Schlichting waves as they undergo rapid distortion

By XUESONG WU[1,2] AND LINDA W. HOGG[1]

[1]Department of Mathematics, Imperial College London, 180 Queens Gate, London SW7 2BZ, UK

[2]Department of Mechanics, Tianjin University, PR China

(Received 20 March 2005 and in revised form 7 September 2005)

This paper is primarily concerned with acoustic radiation of instability waves as they undergo rapid distortion, which is one of the fundamental mechanisms by which instability modes generate sound in subsonic flows. To fix the idea, we consider the case where the abrupt distortion is associated with scattering of a Tollmien–Schlichting (T-S) wave by the mean flow induced by a localized surface roughness in a compressible subsonic boundary layer with an $O(1)$ free-stream Mach number. The sound field was calculated by extending the asymptotic approach based on the triple-deck formalism, developed previously. This approach allows us to identify and approximate the sound source systematically by seeking the solution for the near field hydrodynamics as an asymptotic series in ascending powers of $\epsilon = R^{-1/8}$, where R is the Reynolds number at the roughness site. It is found that the first four terms in the expansion act as octupole, quadrupole, dipole and monopole, respectively, and they make equal order-of-magnitude contributions to the acoustic far field. Some rather delicate source cancellations are noted. As a by-product, the analysis also shows that a localized roughness also influences the energetics of the T-S wave, and that effect can be characterized by a transmission coefficient, defined as the ratio of the T-S wave amplitude after the scattering to that before the scattering.

1. Introduction

The proposition that instability waves, or more broadly, the so-called large-scale coherent structures, could be an important source of sound has attracted much attention for two reasons. (i) Associating sound generation with such clearly identifiable and relatively well-defined physical entities would help clarify the nature of the central concept in Lighthill's (1952) acoustic analogy theory, the quadrupole source, which is in fact a drastic abstraction of the flow information that may be crucial, but not readily available. (ii) Since the instability waves or coherent structures alike can be easily manipulated by various artificial excitations, ample opportunities for noise reduction may arise.

The idea was first suggested by a number of investigators in the 1970s, including Tam (1971, 1972) and Bishop, Ffowcs Williams & Smith (1971) among others, in their efforts to understand the noise-production mechanisms in supersonic jets. A supersonic jet can support the so-called supersonic instability modes, which propagate supersonically relative to the sound speed in the ambient air. These modes radiate highly directional sound in the form of Mach waves, a phenomenon that can be explained easily in terms of the 'wavy-wall analogy' (Tam 1995). The fundamental mechanism of Mach wave radiation was confirmed by the experiments (McLaughlin,

Morrison & Troutt 1975; Troutt & McLaughlin 1982), in which the instability modes were introduced in a controlled manner. Tam & Burton (1984*a*, *b*) formulated an asymptotic theory to calculate the sound radiated by a linearly evolving supersonic mode, and their theoretical prediction was found to be in quantitative agreement with the experimental data. Wu (2005) considered Mach wave radiation by nonlinear evolving supersonic waves or wavetrains. By taking advantage of the fact that the time and length scales characterizing the phase and envelope of the Mach wave are asymptotically distinct, he was able to express the solution explicitly in terms of the amplitude of the instability mode. The resulting solution provides further analytical insight into the structure of the radiated Mach wave beam, and extends the 'wavy-wall analogy', which explains phase propagation only, to illustrate how the envelope propagates.

In the supersonic regime, the concept of instability waves as a dominant source of noise has been accepted, and Mach wave radiation, as a fundamental mechanism, underpins much of our current understanding of noise generation in supersonic turbulent jets; see the review by Tam (1995). In contrast, in the subsonic regime, the role of instability waves in noise generation remains a topic of debate. Following the discovery of orderly structures in subsonic jets (Crow & Champagne 1971), Crow (1972) suggested that these structures might be related to sound emission. Extensive measurements of both instability wave characteristics and the associated acoustic pressure fluctuations were carried out by Moore (1977). He observed that a small pure-tone excitation led to a marked increase in the radiated broadband noise, in agreement with the earlier measurements of Bechert & Pfizenmaier (1975). However, Moore found no evidence for direct sound radiation from the fundamental instability wave and thus concluded that the enhanced sound was due to the instability waves influencing the turbulent mixing.

The role of instability waves in sound production was subsequently studied by Kibens (1980) and Laufer & Yen (1983) in low-Mach-number jets. Their measurements showed that the strong peak in the far-field pressure coincided with the frequencies of the subharmonics (the appearance of which is associated with repeated vortex pairing). Laufer & Yen (1983) noted that there was no Doppler shift in frequency, indicating that the dominant source is at fixed positions, which they identified as the locations of vortex paring. They also found that the sound exhibits superdirectivity and its intensity has a nonlinear (quadratic) dependence on the velocity fluctuation within the shear layer. Since their work, it has been generally accepted that vortex pairing is one of the primary processes responsible for the emission of dominant low-speed jet noise (Zaman 1985). However, Bridges & Hussain (1992) cast some doubt on such an assertion. Their measurement also yielded a drastically different directivity, including an angle of silence (extinction) absent in Laufer & Yen's (1983) experiments. Sound generation by vortex pairing was studied by Mitchell, Lele & Moin (1999) using direct numerical simulation (DNS) at low Reynolds numbers (about 1/20 of that in experiments). Their results predict an angle of silence, somewhat similar to Bridges & Hussain's (1992) measurement, but the reason for the striking disagreement mentioned above remains to be fully understood.

There are two fundamental theoretical approaches for predicting the sound generated by unsteady fluid motions. The first is Lighthill's (1952) acoustic analogy theory and its numerous variants (Phillips 1960; Lilley 1974; Howe 1975). This approach arranges the Navier–Stokes equations to obtain some form of forced wave equations. The 'inhomogeneous' terms are then interpreted as the (equivalent) source of sound. Usually, the source has to be provided by a separate calculation beforehand, and once

this is done, the problem of aeroacoustics becomes one of conventional acoustics. The second and alternative approach, developed independently by Crow (1970), Obermeier (1967) and others, formulates aerodynamic generation of sound as a singular perturbation problem, involving a hydrodynamic motion in the near field and acoustic motion in the far field. The latter is determined by matched asymptotic expansion. This approach treats the source as an integral part of the problem, and has proved to be particularly suitable for calculating the sound radiated by predominantly inviscid vortex motions (e.g. Kambe 1986).

Both Lighthill's theory and the asymptotic approach have been used to estimate the sound emitted by instability waves. The first attempt was made by Crow (1972) for an instability wave in a jet using acoustic analogy theory. He argued that in the vicinity of its saturation (neutral) location, the wave experiences growth followed by decay so that it may be represented by a modulating wave with a Gaussian envelope. We may then propose a quadrupole source which modulates similarly. Such a model was further explored and extended by Ffowcs Williams & Kempton (1978) by including random frequency modulation. It is unclear whether their model viewed the relevant source as due to the interaction of the instability wave with itself or with the background flow, since the amplitude of the source scaled with the square of the fluctuation, yet its frequency was the same as (rather than double) that of the wave. Despite such ambiguity and arbitrariness, a result of general validity is that the magnitude of the radiated sound was determined by the length scale characterizing the wave envelope: the smaller the length scale is, the stronger the sound. It is also noted that the emitted sound is sensitive to the detailed form of the envelope. Ffowcs Williams & Kempton also considered sound radiation by vortex pairing, which was modelled, in a rather arbitrary fashion, by a 'switch over' from a sinusoidal wave to its first subharmonic.

Crighton & Huerre (1990) analysed how the directivity of the acoustic field radiated by a wavepacket is affected by the compactness of the source. Unlike the studies of Crow (1972) and Ffowcs Williams & Kempton (1978), they adopted a boundary-value formulation, where the pressure is governed by a homogeneous wave equation with the source being specified on the boundary. In addition to confirming the sensitivity of the radiated sound to the detailed form of the envelope, as noted earlier by Ffowcs Williams & Kempton (1978), their analysis revealed further that for the source to be compact, the wavelength of sound has to be much larger than the so-called 'penetration length' of the hydrodynamics motion; the latter is usually much longer than the length scale of the envelope. When the compactness condition is violated, the acoustic field cannot be represented by multipoles. As a result, the directivity exhibits an exponential dependence on the cosine of the emission angle, as opposed to the algebraic dependence that is characteristic of sound fields of the multipolar type. The magnitude of the sound, on the other hand, is found to be exponentially small.

While the theoretical models mentioned above have captured some relevant features of the acoustic radiation of a modulated wavepacket or wavetrain, they are all far from being a truthful description of the physical problem since the basic flow that supports the instability wavepacket has been completely ignored, and as a result, the source terms were prescribed rather arbitrarily. An important step to overcome this shortcoming was taken by Tam & Morris (1980), who used a multiple-scale method to describe the streamwise development of a linearly developing (inviscid Rayleigh) instability wave on a spatially varying shear layer. They showed that the straightforward asymptotic expansion for the instability wave is not uniformly valid across the whole flow, because the high-order terms develop a secular behaviour. An outer region accommodating the acoustic motion has to be introduced to render the solution uniformly valid.

The instability wave acts as a driving force for the acoustic fluctuation and the latter was determined by matching. Huerre & Crighton (1983) derived an envelope equation that properly describes the evolution of an instability wave, but they used Lighthill's acoustic analogy to calculate the radiated sound. The source was explicitly assumed to be associated with the wave interacting with the mean shear (cf. Ffowcs Williams & Kempton 1978). The resulting directivity exhibited an angle of silence that was not observed in Laufer & Yen's (1983) experiments. The linear nature of the assumed source means that the theory was deemed unable to account for the observed scaling relation of the sound intensity. The disagreements led Huerre & Crighton (1983) to cast some doubt on Lighthill's version of acoustic analogy, and to suggest that a different form of analogy (Lilley 1974) might be required to account for the 'flow shielding' effect.

Rayleigh waves originate from inviscid instability. Tollmien–Schlichting (T-S) waves represent a different type of instability which is viscous in its origin. The sound emission by such a linear wave in a Blasius boundary layer has been studied by Akylas & Toplosky (1985), using essentially the same asymptotic approach as Tam & Morris (1980). Later, Haj-Hariri & Akylas (1986) considered the acoustic radiation of nonlinear T-S wavepackets, generated by line or point disturbances on a marginally stable asymptotic suction boundary layer. Wang, Lele & Moin (1996) investigated the acoustic radiation during boundary-layer transition. The DNS data of spatial transition was used to calculate the source term in Lighthill's acoustic analogy. They found that sound waves were mainly emitted during the breakdown of the detached high shear layer into small-scale motions.

All the theoretical investigations mentioned above are concerned with instability waves that are undergoing *slow distortion*, in the sense that the waves modulate over a length scale much longer than their wavelengths. As has been indicated already, such waves, in fact, produce very little sound. This is not surprising since the energy carried by such wavepackets concentrates in the Fourier components with wavenumbers close to that of the carrier wave. These energetic components, however, do not radiate because their phase speeds are in the subsonic range. Only the components with sufficiently small wavenumbers are radiating, but the energy carried by them is very small, and indeed very often exponentially small.

Strong radiation occurs when an instability wave undergoes abrupt distortion. It is known that the spreading rate of an artificially excited shear layer undergoes sudden changes at the discrete locations where successive vortex pairing takes place (Ho & Huang 1982). Thus, the fundamental and subharmonic components of a Rayleigh instability wave will be scattered at these locations. A theoretical model for the sound radiated by this mechanism, which obviously is quite different from that of Ffowcs Williams & Kempton (1978), was proposed by Goldstein (1984). In the small-Mach-number limit, Goldstein calculated the sound produced using the matched asymptotic expansion technique.

An extreme case of rapid distortion of instability waves occurs when they interact with a trailing edge, where the sudden change of boundary condition causes an abrupt mean-flow variation to produce a strong scattering effect. Experiments show that instability waves in the oncoming boundary layer are scattered to generate a substantial amount of sound and thus constitute a dominant source of the total airframe noise (e.g. Arbey & Bataille 1983; Nash & Lowson 1999). The mechanism, however, cannot be described by existing trailing-edge noise theory (Howe 1976, 1978) or the 'excess jet noise' model (Munt 1977, Cargill 1982), simply because, in all these models, the upstream flow field is assumed to be uniform and hence cannot support any instability wave. We note that since both the mean-flow distortion and

the T-S wave can be described by triple-deck theory, an asymptotic theory for the present trailing-noise generation mechanism can be constructed by using the same framework. Unfortunately, the resulting system would have to be solved numerically.

In the present paper, we study instead the sound generation as a T-S wave interacts with the rapidly varying steady flow induced by a localized surface roughness. This scenario is of some practical relevance as it may be another potential contribution to the airframe noise. A shared feature with the trailing-edge noise problem described above is that the T-S wave undergoes *rapid distortion*, in the sense that the wave magnitude experiences a significant change over one wavelength. Therefore, a study of this problem may lead to an insight into a fundamental mechanism by which instability waves radiate sound, even though the discontinuity associated with the edge may present a significant difference.

Mathematically, the present problem has the advantage that it can be described and solved in a completely self-consistent manner by adopting the asymptotic approach developed by Wu (2002). Unlike the acoustic analogy, this approach describes the radiation process directly, i.e. it examines how the hydrodynamic motion evolves to acquire the character of sound in the far field, which is the only way that leads to systematic identification of the true acoustic sources, without the ambiguity and arbitrariness that plague the acoustic analogy type of approach.

The rest of the paper is structured as follows. In § 2, the problem is formulated, and the relevant scalings are specified so that both the T-S wave and the mean flow induced by the roughness can be described by triple-deck theory. The linearized solution for the steady flow is presented in § 2.1, while the oncoming T-S wave is specified in § 2.2. The T-S wave interacts with the mean-flow distortion to produce a scattered field, which is governed by inhomogeneous triple-deck systems with the forcing coming both from the Reynolds stresses and boundary conditions. The solution can be expanded in the ascending powers of $R^{-1/8}$, and the first four terms in the expansion are obtained in § 3. The large-distance asymptotic behaviour of the pressure in the upper layer shows that the first four terms in the solution contribute octupole, quadrupole, dipole and monopole sources, respectively, to the sound generation (§ 4). The expansion in the upper layer becomes disordered in the far field, where the motion becomes acoustic in nature. An outer acoustic region must be considered, where the pressure is governed by the conventional convected wave equation in a uniformly moving medium. The relevant solution can be represented by a linear superposition of octupole, quadrupole, dipole and monopole, with the combination coefficients being determined by matching with the solution in the upper deck. The formula for the intensity and directivity of the radiated sound can be given in the closed form. In § 5, we show that the instability wave may, on interacting with the localized roughness, be energized or weakened. This can be measured appropriately by a transmission coefficient. Results of the relevant parametric study are presented in § 6, and a summary and some concluding remarks are given in § 7.

2. Formulation and scalings

We consider the two-dimensional compressible boundary layer over an airfoil. An isolated surface roughness is located at a distance l from the leading edge. A two-dimensional T-S wave, excited by some receptivity mechanism at some location upstream of the roughness, propagates within the boundary layer in the streamwise direction. It decays exponentially in the transverse direction. However, as the wave interacts with the sudden mean-flow variation induced by the roughness, it produces

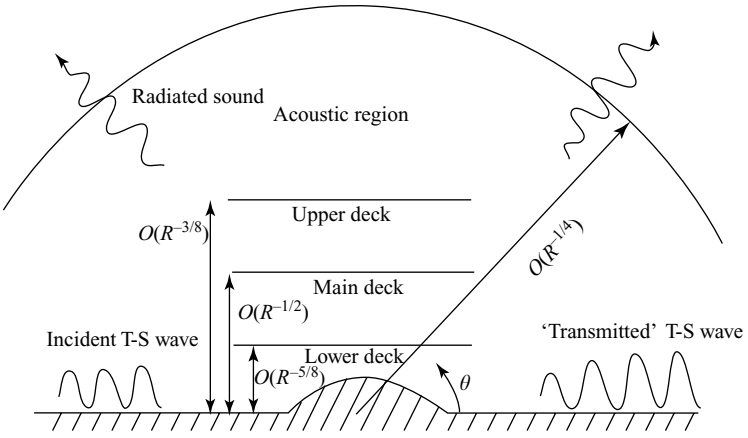

FIGURE 1. A sketch of the flow structure illustrating the scattering and radiation processes.

a scattered field, the far field of which decays only algebraically and in fact represents the propagation of sound (figure 1). The aim of the present study is to calculate this sound field.

Let U_∞ denote the local inviscid slip velocity at the top of the roughness element. The mean density, temperature, viscosity and sound speed in the free stream are denoted by ρ_∞, T_∞, μ_∞ and a_∞, respectively. We define the Mach number M and the Reynolds number R as

$$M = U_\infty/a_\infty, \quad R = U_\infty l/\nu_\infty, \tag{2.1}$$

where $\nu_\infty = \mu_\infty/\rho_\infty$ is the kinematic viscosity. The focus will be on the subsonic flow with $M < 1$ being of $O(1)$. The Reynolds number is taken to be asymptotically large, $R \gg 1$.

We introduce a Cartesian coordinate system (x_1, x_2) with its origin at the centre of the roughness element, where x_1 and x_2 are along and normal to the surface; they are non-dimensionalized by l. The time variable t is normalized by l/U_∞. The velocity $\boldsymbol{u} = (u, v)$, density ρ and temperature τ are non-dimensionalized by U_∞, ρ_∞ and T_∞, respectively, while the non-dimensionalized pressure p is introduced by writing the dimensional pressure as $p_\infty + \rho_\infty U_\infty^2 p$ with p_∞ being a constant.

For simplicity, the fluid is taken to be a perfect gas with a constant ratio of specific heats, γ. The governing equations of the flow are

$$\frac{\partial \rho}{\partial t} + \nabla\cdot(\rho\,\boldsymbol{u}) = 0, \tag{2.2}$$

$$\rho\frac{\mathrm{D}\,\boldsymbol{u}}{\mathrm{D}t} = -\nabla p + \frac{1}{R}\nabla\cdot(2\mu\,\boldsymbol{e}) + \frac{1}{R}\nabla\big(\big(\mu' - \tfrac{2}{3}\mu\big)\nabla\cdot\boldsymbol{u}\big), \tag{2.3}$$

$$\rho\frac{\mathrm{D}\tau}{\mathrm{D}t} = (\gamma-1)M^2\frac{\mathrm{D}p}{\mathrm{D}t} + \frac{1}{PrR}\nabla\cdot(\mu\nabla\tau) + \frac{(\gamma-1)M^2}{R}\Phi, \tag{2.4}$$

$$1 + \gamma M^2 p = \rho\tau, \tag{2.5}$$

where $\boldsymbol{e}$ and Φ represent the tensor of the strain rate and the dissipation function:

$$e_{ij} = \frac{1}{2}\left(\frac{\partial u_i}{\partial x_j} + \frac{\partial u_j}{\partial x_i}\right), \quad \Phi = 2\mu\,\boldsymbol{e}:\boldsymbol{e} + \big(\mu' - \tfrac{2}{3}\mu\big)(\nabla\cdot\boldsymbol{u})^2.$$

The operators such as ∇ are defined with respect to (x_1, x_2), and Pr is the Prandtl number. The shear viscosity μ is assumed to obey the Chapman viscosity law, $\mu = C\tau$, where C is unity for the normalization adopted above (and so will not appear hereinafter). The bulk viscosity plays no role in the order of approximation (and is usually taken to be zero by the Stokes hypothesis).

To describe the boundary-layer flow, we introduce

$$(x, y) = \left(x_1, R^{1/2}x_2\right).$$

The unperturbed basic flow can be written as $(u, v, p, \rho, \tau) = (U_B, R^{-1/2}V_B, P_B, R_B, T_B)$. We shall assume that the wall is adiabatic and the Prandtl number Pr is unity. The temperature profile, $T_B(y)$, is then related to $U_B(y)$ via

$$T_B = 1 + \tfrac{1}{2}(\gamma - 1)M^2\left(1 - U_B^2\right),$$

from which it follows the wall temperature $T_w/T_\infty = 1 + (\gamma - 1)M^2/2$. The state equation and the fact that $P_B = P_B(x)$ yield the relation

$$R_B T_B = 1 + \gamma M^2 P_B.$$

In general, the basic velocity profile has to be obtained numerically by solving the steady boundary-layer equations, but there exists a compressible version of the Falkner–Skan similarity solution for the special case of a flat plate, or if the velocity and temperature at the outer edge of the boundary layer, $U_e(x)$ and $T_e(x)$, satisfy (Stewartson 1974)

$$U_e^2/T_e = (1 + X)^{2m}, \tag{2.6}$$

where the variable X is related to x via the transformation

$$X = \int^x \left(1 + \gamma M^2 P_B(x)\right) T_e^{1/2}(x)\,\mathrm{d}x.$$

The similarity solution then takes form

$$U_B = (1 + X)^m f'(\eta) \quad \text{with} \quad \eta = \left(\frac{1+m}{(1+X)^{(1-m)}}\right)^{1/2} \int_0^y R_B\,\mathrm{d}y;$$

the function f satisfies the equation

$$f''' + \tfrac{1}{2}ff'' + \beta_H(1 - f'^2) = 0 \tag{2.7}$$

and the boundary conditions $f(0) = f'(0) = 0$, $f(\infty) = 0$, where $\beta_H = m/(1+m)$. Since the flow physics concerned is local, occurring in the vicinity of $x = 0$, we can view (2.7) as approximating a local profile with an effective Hartree parameter β_H characterizing the local pressure gradient. In this sense, the restriction of a special global slip velocity distribution (2.6) can be lifted. This is the viewpoint that we shall take in the present paper. Note that the non-dimensionalization based on the local slip velocity and temperature means that $P_B \sim O(x)$ for $x \ll 1$. In what follows, we can take $X \approx x$ for the required approximation. As $y \to 0$,

$$U_B(y) \to \lambda\left(\frac{T_w}{T_\infty}\right)^{-1} y - \tfrac{1}{2}m\left(\frac{T_w}{T_\infty}\right)^{-2} y^2 + \tfrac{1}{6}(\gamma - 1)M^2\lambda^3\left(\frac{T_w}{T_\infty}\right)^{-4} y^3 + \lambda_4 y^4 + O(y^5),$$

where λ is the local skin friction, which in the case of the Falkner–Skan similarity solution is given by $\lambda = \lambda_0(1 + X)^{-(1-m)/2}$ with $\lambda_0 \equiv (1 + m)^{1/2} f''(0)$ being a constant. The (unwieldy) expression for λ_4 is not required.

Since $T_B R_B \approx 1$, it follows that

$$R_B \to \left(\frac{T_w}{T_\infty}\right)^{-1} + \tfrac{1}{2}(\gamma-1)M^2\lambda^2\left(\frac{T_w}{T_\infty}\right)^{-4} y^2 - \tfrac{1}{2}(\gamma-1)M^2\lambda m\left(\frac{T_w}{T_\infty}\right)^{-5} y^3 + O(y^4).$$

The total flow field consists of the steady boundary-layer flow, and a (small) perturbation, that is

$$(u, v, p, \rho, \tau) = \left(U_B, R^{-1/2}V_B, P_B, R_B, T_B\right) + (\tilde{u}, \tilde{v}, \tilde{p}, \tilde{\rho}, \tilde{\tau}). \tag{2.8}$$

Substitution of (2.8) into (2.2)–(2.5) yields the perturbation equations, which to the required order of approximation, can be written as

$$\tilde{\rho}_t + U_B\tilde{\rho}_x + R_B\tilde{u}_x + \epsilon^{-4}(R_B\tilde{v}_y + R_{B,y}\tilde{v}) = N_c, \tag{2.9}$$

$$R_B(\tilde{u}_t + U_B\tilde{u}_x + \epsilon^{-4}U_{B,y}\tilde{v}) = -\tilde{p}_x + (T_B\tilde{u}_y)_y + (U_{B,y}\tilde{\tau})_y + N_u, \tag{2.10}$$

$$R_B(\tilde{v}_t + U_B\tilde{v}_x) = -\epsilon^{-4}\tilde{p}_y + 2(T_B\tilde{v}_y)_y + \epsilon^4(T_B\tilde{u}_y)_x + N_p, \tag{2.11}$$

$$\begin{aligned} R_B(\tilde{\tau}_t + U_B\tilde{\tau}_x + \epsilon^{-4}T_{B,y}\tilde{v}) &= (\gamma-1)M^2(\tilde{p}_t + U_B\tilde{p}_x) + (T_B\tilde{\tau}_y)_y + (T_{B,y}\tilde{\tau})_y \\ &\quad + 2(\gamma-1)M^2T_BU_{B,y}\tilde{u}_y + N_\tau, \end{aligned} \tag{2.12}$$

$$\gamma M^2\tilde{p} = T_B\tilde{\rho} + R_B\tilde{\tau} + \tilde{\rho}\tilde{\tau}, \tag{2.13}$$

where we have defined the small parameter

$$\epsilon = R^{-1/8},$$

and the nonlinear terms are given by

$$\begin{aligned} N_c &= -((\tilde{\rho}\tilde{u})_x + \epsilon^{-4}(\tilde{\rho}\tilde{v})_y), \\ N_u &= -R_B(\tilde{u}\tilde{u}_x + \epsilon^{-4}\tilde{v}\tilde{u}_y) + \tilde{\rho}\tilde{p}_x/R_B, \quad N_p = -R_B(\tilde{u}\tilde{v}_x + \epsilon^{-4}\tilde{v}\tilde{v}_y) + \epsilon^{-4}\tilde{\rho}\tilde{p}_y/R_B, \\ N_\tau &= -R_B(\tilde{u}\tilde{\tau}_x + \epsilon^{-4}\tilde{v}\tilde{\tau}_y) + (\gamma-1)M^2\left((\tilde{u}\tilde{p}_x + \epsilon^{-4}\tilde{v}\tilde{p}_y) - \tilde{\rho}(\tilde{p}_t + U_B\tilde{p}_x)/R_B\right). \end{aligned}$$

In (2.9)–(2.12), we have ignored (i) the momentum and thermal diffusion in the streamwise direction, and (ii) all the terms in the dissipation function except the leading-order one. There are also terms involving V_B and the streamwise derivatives of the mean-flow quantities (such as $U_{B,x}$, $T_{B,x}$ etc.), which represent the non-parallel-flow effect. They affect the last term in the expansion for the hydrodynamic motion, but their contribution to the far field sound is negligible, and hence, for brevity, these terms are not written out.

Equations (2.12) and (2.13) are combined to give

$$(\tilde{\rho}_t + U_B\tilde{\rho}_x) + \epsilon^{-4}R_{B,y}\tilde{v} = R_BM^2(\tilde{p}_t + U_B\tilde{p}_x) + T_B^2\tilde{\rho}_{yy} - 2(\gamma-1)M^2U_{B,y}\tilde{u}_y + N_\rho, \tag{2.14}$$

where

$$N_\rho = -R_B(\partial_t + U_B\partial_x)(\tilde{\rho}\tilde{\tau}) - R_BN_\tau.$$

Equation (2.10) can be rewritten, on replacing $\tilde{\tau}$ using the state equation (2.13), as

$$R_B(\tilde{u}_t + U_B\tilde{u}_x + \epsilon^{-4}U_{B,y}\tilde{v}) = -\tilde{p}_x + (T_B\tilde{u}_y)_y + (U_{B,y}T_B(\gamma M^2\tilde{p} - T_B\tilde{\rho} - \tilde{\rho}\tilde{\tau}))_y + N_u. \tag{2.15}$$

Equations (2.9), (2.11) and (2.14)–(2.15) form the system governing the total perturbation, $(\tilde{\boldsymbol{u}}, \tilde{p}, \tilde{\rho}, \tilde{\tau})$, which can be decomposed as

$$(\tilde{\boldsymbol{u}}, \tilde{p}, \tilde{\rho}, \tilde{\tau}) = (\boldsymbol{u}_m, p_m, \rho_m, \tau_m) + (\boldsymbol{u}_I, p_I, \rho_I, \tau_I) + (\tilde{\boldsymbol{u}}_s, \tilde{p}_s, \tilde{\rho}_s, \tilde{\tau}_s), \tag{2.16}$$

where quantities with subscripts m, I and s refer to the local mean-flow distortion, the incident T-S wave and the scattered field, respectively.

The T-S wave is assumed to have a wavelength comparable with the length scale of the inhomogeneity (i.e. the local mean-flow distortion), and so it undergoes rapid distortion during scattering. The mechanism of acoustic radiation could be readily understood in the spectrum space. Suppose that the T-S wave has a wavenumber α. The mean-flow distortion has a continuous Fourier spectrum, which is a continuous function of wavenumber k. The interaction between them generates components with wavenumbers $(k-\alpha)$. The majority of the components with $(k-\alpha)=O(1)$ are non-radiating, since their phase speeds are subsonic. Only the long-wavelength components with $(k-\alpha)\ll 1$ have supersonic phase speeds relative to the sound speed in the free stream, and they emit acoustic waves to the far field. The intensity of the emitted sound wave is proportional to the amplitude of the Fourier component with the wavenumber α, which is among the primary energy-containing components because the mean-flow distortion has a length scale comparable with α^{-1}. Strong radiation is therefore expected.

The sound generated by scattering will be calculated by extending the systematic asymptotic approach based on the triple-deck formalism, developed in a previous paper (Wu 2002). This approach is natural for the problem under consideration because the triple-deck structure governs both ingredients of the acoustic source: the T-S wave (Smith 1979, 1989) and the mean-flow distortion (Smith 1973). The same structure describes the scattering process. The unsteady motion induced by scattering is of a hydrodynamic nature in the lower, main and upper decks, but it acquires the character of sound in the far field. Therefore, an outer acoustic region has to be introduced (figure 1), in addition to the standard three decks, which will be referred to collectively as the hydrodynamic region. We introduce the characteristic faster spatial and temporal variables in triple-deck theory

$$\bar{x} = R^{3/8}\Omega^3 x, \quad \bar{t} = R^{2/8}\Omega^3 t, \tag{2.17}$$

where $\Omega = (T_w/T_\infty)^{-1/2}$, and the renormalization factor Ω^3 is inserted for convenience.

2.1. *The mean-flow distortion*

The surface roughness is assumed to have a height of $O(R^{-5/8}l)$ or smaller, and a streamwise length scale of $O(R^{-3/8}l)$. The resulting mean-flow distortion is governed by a triple-deck structure, as was shown by Smith (1973). The viscous effect is confined in a region $Y = O(1)$, where

$$Y = R^{1/8}\Omega^3 y.$$

In terms of the variable Y, the shape of the roughness is described by

$$Y = hF_w(\bar{x}). \tag{2.18}$$

When $h = O(1)$, the flow in the lower deck will be governed by the fully nonlinear boundary-layer equations. In the present study, we assume that $h \ll O(1)$ so that the governing equations can be linearized and the solution can be obtained analytically by using a Fourier transform with respect to $\bar{x}$. Let $\widehat{F}(k)$ denote a Fourier transform of $F_w(\bar{x})$, i.e.

$$\widehat{F}(k) = \frac{1}{(2\pi)^{1/2}} \int_{-\infty}^{\infty} F_w(\bar{x})\, \mathrm{e}^{-\mathrm{i}k\bar{x}}\, \mathrm{d}\bar{x}.$$

Since for calculating the radiated sound, it is the Fourier transform that is required, the mean-flow solution will be presented in the Fourier spectral space.

Consider the main part of the boundary layer first. It is convenient to use the re-normalized variable

$$\tilde{y} = \Omega^2 y.$$

For $\tilde{y} = O(1)$, the mean-flow distortion due to the surface roughness is a small perturbation to the base-flow profile $(U_B, R^{-1/2}V_B)$. The Fourier transform of this mean-flow distortion expands as

$$\left.\begin{aligned} u_m &= \epsilon h \Omega^{-1}\big(U_m^{(1)}(\tilde{y},k) + \epsilon U_m^{(2)} + \epsilon^2 U_m^{(3)} + \cdots\big),\\ v_m &= \epsilon^2 h\big(V_m^{(1)}(\tilde{y},k) + \epsilon V_m^{(2)} + \epsilon^2 V_m^{(3)} + \cdots\big),\\ p_m &= \epsilon^2 h\big(P_m^{(1)}(\tilde{y},k) + \epsilon P_m^{(2)} + \epsilon^2 P_m^{(3)} + \cdots\big),\\ \rho_m &= \epsilon h \Omega^{-1}\big(R_m^{(1)}(\tilde{y},k) + \epsilon R_m^{(2)} + \epsilon^2 R_m^{(3)} + \cdots\big). \end{aligned}\right\} \tag{2.19}$$

Throughout this paper, the logarithmic terms such as $\epsilon^n \ln\epsilon$ are tactically (and conveniently) absorbed into $O(\epsilon^n)$ terms. It turns out that in order to obtain the leading-order approximation for the radiated sound, it is necessary to consider the solution for the mean-flow distortion up to $O(\epsilon)$. This is because there is a rather delicate cancellation in the sources (i.e. Reynolds stress) associated with the leading-order interaction between the T-S wave and mean-flow distortion, leading to reduced acoustic efficiency. As will be shown in § 4, the leading-order interaction within the lower deck generates the Reynolds stress of the largest magnitude, but as a result of cancellation in the small-wavenumber limit, it acts as an acoustic octupole rather than a quadrupole as we might expect. Similarly, in the main deck, the leading-order interaction acts as a quadrupole. It is necessary to check whether the high-order interactions contribute acoustic multipoles of lower order.

The leading-order perturbation satisfies the familiar equations (Stewartson 1974)

$$\left.\begin{aligned} \mathrm{i}k\big(R_B U_m^{(1)} + U_B R_m^{(1)}\big) + \big(R_B V_m^{(1)}\big)_{\tilde{y}} &= 0,\\ \mathrm{i}k U_B U_m^{(1)} + U_B' V_m^{(1)} &= 0,\\ \mathrm{i}k U_B R_m^{(1)} + R_B' V_m^{(1)} &= 0, \end{aligned}\right\} \tag{2.20}$$

which have the solution

$$U_m^{(1)} = A_m^{(1)} U_B', \quad V_m^{(1)} = -\mathrm{i}k A_m^{(1)} U_B, \quad R_m^{(1)} = A_m^{(1)} R_B', \tag{2.21}$$

where $A_m^{(1)}(k)$ is a function of k to be determined later. The leading-order temperature in the spectral space is obtained through the state equation as $\tau_m^{(1)} = -A_m^{(1)} R_B'/R_B^2 = -R_m^{(1)}/R_B^2$.

We can readily write down the governing equations for the second-order perturbation. Omitting the details for brevity, we give only the final solution,

$$\left.\begin{aligned} V_m^{(2)} &= \mathrm{i}k U_B\left[-A_m^{(2)} + \Omega P_m^{(1)}\int^{\tilde{y}}\left(\frac{1}{R_B U_B^2} - M^2\right)\mathrm{d}\tilde{y}\right],\\ U_m^{(2)} &= -\frac{\Omega P_m^{(1)}}{R_B U_B} - U_B'\left[-A_m^{(2)} + \Omega P_m^{(1)}\int^{\tilde{y}}\left(\frac{1}{R_B U_B^2} - M^2\right)\mathrm{d}\tilde{y}\right],\\ R_m^{(2)} &= \Omega P_m^{(1)} M^2 R_B - R_B'\left[-A_m^{(2)} + \Omega P_m^{(1)}\int^{\tilde{y}}\left(\frac{1}{R_B U_B^2} - M^2\right)\mathrm{d}\tilde{y}\right],\\ P_m^{(2)} &= \tilde{P}_m^{(2)} - k^2 A_m^{(1)}\Omega\int_0^{\tilde{y}} R_B U_B^2\,\mathrm{d}\tilde{y}, \end{aligned}\right\} \tag{2.22}$$

where $A_m^{(2)}$ and $\tilde{P}_m^{(2)}$ are functions of k to be found. The second-order temperature is given by

$$\tau_m^{(2)} = -R_m^{(2)}/R_B^2 - \Omega\gamma M^2 P_m^{(1)}/R_B.$$

It is easy to show that as $\tilde{y} \to \infty$,

$$\left.\begin{aligned} V_m^{(2)} &\sim \Omega\left(\mathrm{i}kP_m^{(1)}\right)(1-M^2)\tilde{y} + \left(-\mathrm{i}kA_m^{(2)} + \Omega\mathrm{i}kP_m^{(1)}J_\infty\right) + \cdots, \\ P_m^{(2)} &\sim \left(-\Omega k^2 A_m^{(1)}\right)\tilde{y} + \left(\tilde{P}_m^{(2)} - \Omega k^2 A_m^{(1)} I_2\right) + \cdots, \end{aligned}\right\} \tag{2.23}$$

whereas $\tilde{y} \to 0$,

$$U_m^{(2)} \sim (\lambda_2/\lambda^2)P_m^{(1)}\ln\tilde{y} + \left(\lambda A_m^{(2)} - \Omega\lambda J_0 P_m^{(1)} + \tfrac{3}{2}(\lambda_2/\lambda^2)P_m^{(1)}\right) + \cdots, \tag{2.24}$$

where $\lambda_2 = -\Omega^{-1}\beta_H/(1-\beta_H)$, and J_∞, J_0 and I_2 are defined by (A 4), (A 3) and (A 1), respectively.

In the upper deck, the local transverse variable is

$$\bar{y} = R^{-1/8}\Omega\tilde{y}.$$

The steady-flow distortion is a small perturbation to the (local) uniform flow. The Fourier transforms of its velocity, pressure and density have the expansion

$$(\boldsymbol{u}_m, p_m, \rho_m) = \epsilon^2 h\left\{\left(\boldsymbol{u}_m^{(1)}, \bar{p}_m^{(1)}, \bar{\rho}_m^{(1)}\right) + \epsilon\left(\boldsymbol{u}_m^{(2)}, \bar{p}_m^{(2)}, \bar{\rho}_m^{(2)}\right) + \cdots\right\}. \tag{2.25}$$

The governing equations for $\bar{p}_m^{(j)}$ and $\bar{v}_m^{(j)}$ $(j = 1, 2)$ are

$$\bar{p}_{m,\bar{y}\bar{y}}^{(j)} - (1-M^2)k^2\bar{p}_m^{(j)} = 0, \quad \mathrm{i}k\bar{\rho}_m^{(j)} + \mathrm{i}k\bar{u}_m^{(j)} + \bar{v}_{m,\bar{y}}^{(j)} = 0, \quad \bar{u}_m^{(j)} = -\bar{p}_m^{(j)}, \quad \mathrm{i}k\bar{v}_m^{(j)} = -\bar{p}_{m,\bar{y}}^{(j)}.$$

It follows that

$$\left(\bar{u}_m^{(j)}, \bar{v}_m^{(j)}, \bar{p}_m^{(j)}, \bar{\rho}_m^{(j)}\right) = (-1, -\mathrm{i}\bar{\kappa}/k, 1, M^2)\bar{P}_m^{(j)}\,\mathrm{e}^{-\bar{\kappa}\bar{y}}, \tag{2.26}$$

where $\bar{\kappa}$ is defined as

$$\bar{\kappa} = (1-M^2)^{1/2}|k| = (1-M^2)^{1/2}[(k+\mathrm{i}0)(k-\mathrm{i}0)]^{1/2};$$

here, $|k|$ denotes an analytic continuation of the usual square root function into the complex plane, with the branch being such that the real part of $|k|$ is always non-negative. The pressure and vertical velocity in the upper deck match their counterparts in the main layer at the first two orders if

$$\bar{P}_m^{(1)} = P_m^{(1)}, \quad P_m^{(1)} = k^2/\bar{\kappa}A_m^{(1)}, \tag{2.27}$$

$$\bar{P}_m^{(2)} = \tilde{P}_m^{(2)} - \Omega k^2 A_m^{(1)} I_2, \quad -\mathrm{i}kA_m^{(2)} + \Omega\mathrm{i}kP_m^{(1)}J_\infty = -\mathrm{i}\bar{\kappa}/k\,\bar{P}_m^{(2)}. \tag{2.28}$$

In the lower deck, where $Y = R^{1/8}\Omega\tilde{y} = O(1)$, the base-flow profile is approximated, to leading term, by $R^{-1/8}\Omega^{-1}\lambda Y$. For $h \ll 1$, the roughness-induced mean flow is a small perturbation to this uniform shear, and its Fourier transform can be expanded as

$$\left.\begin{aligned} (u_m,\ v_m) &= \epsilon h\Omega^{-1}\left(\left(\tilde{U}_m^{(1)}, \epsilon^2\tilde{V}_m^{(1)}\right) + \epsilon\left(\tilde{U}_m^{(2)}, \epsilon^2\tilde{V}_m^{(2)}\right) + \cdots\right), \\ p_m &= \epsilon^2 h\left(P_m^{(1)} + \epsilon\tilde{P}_m^{(2)} + \cdots\right), \\ \rho_m &= \epsilon^2 h\Omega^2\left(\tilde{R}_m^{(1)} + \epsilon\tilde{R}_m^{(2)} + \cdots\right). \end{aligned}\right\} \tag{2.29}$$

The leading- and second-order terms satisfy the linearized boundary-layer equations

$$\left.\begin{aligned} \mathrm{i}k\tilde{U}_m^{(j)} + \tilde{V}_{m,Y}^{(j)} &= 0, \\ \mathrm{i}k\lambda Y\tilde{U}_m^{(j)} + \lambda\tilde{V}_m^{(j)} &= -\mathrm{i}k\tilde{P}_m^{(j)} + \tilde{U}_{m,YY}^{(j)} - \tfrac{1}{2}\lambda_2\left(Y^2\mathrm{i}k\tilde{U}_m^{(1)} + 2Y\tilde{V}_m^{(1)}\right)\delta_{j2}, \end{aligned}\right\} \tag{2.30}$$

for $j = 1, 2$, and δ_{j2} is the Kronecker delta. Also here we put $\tilde{P}_m^{(1)} = P_m^{(1)}$. The no-slip condition at $Y = hF_w$ is approximated, after linearization, by

$$\tilde{U}_m^{(1)}(0) = -\lambda\widehat{F}, \quad \tilde{V}_m^{(1)}(0) = 0; \quad \tilde{U}_m^{(2)}(0) = \tilde{V}_m^{(2)}(0) = 0, \tag{2.31}$$

while matching with the main-deck solutions (see (2.21) and (2.24)) requires that

$$\tilde{U}_m^{(1)} \to \lambda A_m^{(1)}, \quad \tilde{U}_m^{(2)} \to \lambda A_m^{(2)} - \Omega\lambda J_0 P_m^{(1)} + \tfrac{3}{2}(\lambda_2/\lambda^2)P_m^{(1)} \quad \text{as} \quad Y \to \infty. \tag{2.32}$$

After solving equations (2.30) subject to (2.31), and using the matching conditions (2.27), (2.28) and (2.32), the leading-order solution is found to be

$$\tilde{U}_m^{(1)} = \lambda\widehat{F}\left\{\frac{1}{\mathscr{D}(k)}\int_0^\xi \mathrm{Ai}(\xi)\,\mathrm{d}\xi - 1\right\}, \tag{2.33}$$

$$\bar{P}_m^{(1)} = P_m^{(1)} = \tilde{P}_m^{(1)} = -k^{-2}(\mathrm{i}k\lambda)^{5/3}\mathrm{Ai}'(0)\widehat{F}/\mathscr{D}(k), \tag{2.34}$$

where Ai denotes the Airy function, $\xi = (\mathrm{i}k\lambda)^{1/3}Y$, and

$$\mathscr{D}(k) = \int_0^\infty \mathrm{Ai}(\xi)\,\mathrm{d}\xi + \frac{\mathrm{i}\lambda(\mathrm{i}k\lambda)^{2/3}\bar{\kappa}}{k^3}\mathrm{Ai}'(0) = \tfrac{1}{3} - \frac{\mathrm{i}\lambda(\mathrm{i}k\lambda)^{2/3}\bar{\kappa}}{k^3 3^{1/3}\Gamma(1/3)}, \tag{2.35}$$

The second-order solution is

$$\begin{aligned}\tilde{U}_m^{(2)} = {} & \tfrac{1}{2}\lambda_2(\mathrm{i}k\lambda)^{-1/3}\left\{\tfrac{1}{5}[\xi^2\mathrm{Ai}(\xi) - 3\mathrm{Ai}'(\xi) + 3\mathrm{Ai}'(0)](\widehat{F}/\mathscr{D})\right. \\ & \left. + 2\widehat{F}\left[\frac{1}{\mathscr{D}}\int_0^\xi(\xi - \tilde{\xi})\mathrm{Ai}(\tilde{\xi})\,\mathrm{d}\tilde{\xi} - \xi + \frac{\mathrm{Ai}'(0)}{\mathscr{D}}\int_0^\xi M_0(\tilde{\xi})\,\mathrm{d}\tilde{\xi}\right]\right\} + C_m^{(2)}\int_0^\xi \mathrm{Ai}(\xi)\,\mathrm{d}\xi,\end{aligned} \tag{2.36}$$

$$\begin{aligned}\tilde{P}_m^{(2)} = {} & -\frac{\mathrm{i}(\mathrm{i}k\lambda)^{2/3}\mathrm{Ai}'(0)}{k\mathscr{D}(k)}\left\{\Omega\lambda[J_\infty - J_0 - (1-M^2)I_2]P_m^{(1)}\right. \\ & - \tfrac{1}{2}\lambda_2(\mathrm{i}k\lambda)^{-1/3}\left[\left(-\tfrac{2}{5}\mathrm{Ai}'(0) - \tfrac{9}{5}\mathrm{Ai}(0)\mathscr{R}_0\right)\widehat{F}/\mathscr{D}\right. \\ & \left.\left. + 2\mathrm{Ai}'(0)(\widehat{F}/\mathscr{D})\left(\chi_0 - \ln\Omega(\mathrm{i}k\lambda)^{1/3}/\epsilon + \pi\mathrm{Bi}'(0)\mathscr{R}_0\int_0^\infty \mathrm{Ai}(\xi)\,\mathrm{d}\xi\right)\right]\right\},\end{aligned} \tag{2.37}$$

with

$$\begin{aligned}C_m^{(2)} = {} & \frac{1}{\mathscr{D}(k)}\left\{\Omega\lambda[J_\infty - J_0 - (1-M^2)I_2]P_m^{(1)}\right. \\ & - \tfrac{1}{2}\lambda_2(\mathrm{i}k\lambda)^{-1/3}\left[\left(-\tfrac{2}{5}\mathrm{Ai}'(0) + \tfrac{9}{5}\mathrm{Ai}(0)\frac{\mathrm{i}\lambda(\mathrm{i}k\lambda)^{2/3}\bar{\kappa}}{k^3}\right)\widehat{F}/\mathscr{D}\right. \\ & \left.\left. + 2\mathrm{Ai}'(0)\widehat{F}/\mathscr{D}\left(\chi_0 - \ln\Omega(\mathrm{i}k\lambda)^{1/3}/\epsilon - \pi\mathrm{Bi}'(0)\frac{\mathrm{i}\lambda(\mathrm{i}k\lambda)^{2/3}\bar{\kappa}^3}{k}\right)\right]\right\}.\end{aligned}$$

Here we have put $\mathscr{R}_0 = -3^{-2/3}\Gamma(1/3)$, $M_0 = M(\xi, 0)$ with $M(\xi, \xi_0)$ being defined as

$$M(\xi, \xi_0) = \pi\left\{\mathrm{Bi}(\xi)\int_\infty^\xi \mathrm{Ai}(\tilde{\xi})\,\mathrm{d}\tilde{\xi} - \mathrm{Ai}(\xi)\int_{\xi_0}^\xi \mathrm{Bi}(\tilde{\xi})\,\mathrm{d}\tilde{\xi}\right\}, \tag{2.38}$$

and χ_0 is the Hadamard finite part integral

$$\chi_0 = \int_0^\infty \left(M_0(\xi) + \frac{1}{\xi}\right)\mathrm{d}\xi.$$

From the x-momentum equations in (2.30), the vertical velocity components $\tilde{V}_m^{(j)}$ ($j = 1, 2$) are obtained as

$$\tilde{V}_m^{(j)} = \frac{1}{\lambda}\big(\tilde{U}_{m,YY}^{(j)} - \mathrm{i}kY\tilde{U}_m^{(j)} - \mathrm{i}k\tilde{P}_m^{(j)} - \tfrac{1}{2}\lambda_2\big(Y^2\mathrm{i}k\tilde{U}_m^{(1)} + 2Y\tilde{V}_m^{(1)}\big)\delta_{j2}\big). \tag{2.39}$$

The solutions at the next two orders can be obtained. Though these high-order corrections do affect the third- and fourth-order solutions of the scattered field in the hydrodynamic region, they do not alter the far-field behaviour of these solutions so that their contribution to the acoustic radiation is negligible. For the purpose of calculating the leading-order acoustic field, it suffices to use the mean-flow distortion accurate up to $O(\epsilon)$.

2.2. *The incident T-S wave*

Upstream of the roughness, where the mean flow changes slowly over the slow variable x, the unsteady motion is the T-S wave, whose solution is described by an eigenvalue problem. In the main deck, the solution for the T-S wave takes the form (Smith 1989)

$$\left.\begin{aligned} u_I &= \delta\Omega^{-1}(u_1 + \epsilon u_2 + \epsilon^2 u_3 + \cdots)E + \text{c.c.},\\ v_I &= \delta\epsilon(v_1 + \epsilon v_2 + \epsilon^2 v_3 + \cdots)E + \text{c.c.},\\ p_I &= \delta\epsilon(p_1 + \epsilon p_2 + \epsilon^2 p_3 + \cdots)E + \text{c.c.},\\ \rho_I &= \delta\Omega^{-1}(\rho_1 + \epsilon\rho_2 + \epsilon^2\rho_3 + \cdots)E + \text{c.c.}, \end{aligned}\right\} \tag{2.40}$$

where for convenience, we define

$$E = \exp\{\mathrm{i}(\alpha\bar{x} - \omega\bar{t})\},$$

and the wavenumber α expands as

$$\alpha = \alpha_1 + \epsilon\alpha_2 + \epsilon^2\alpha_3 + \cdots. \tag{2.41}$$

For the purpose of obtaining the leading-order solution for the acoustic field, the T-S wave solution to $O(\epsilon)$ has to be considered.

At leading-order, the T-S wave has the familiar solution for its velocity and density

$$u_1 = a_1 U_B', \quad v_1 = -\mathrm{i}\alpha_1 a_1 U_B, \quad \rho_1 = a_1 R_B', \tag{2.42}$$

where the constant a_1 is a measure of the scaled amplitude of the T-S wave. The temperature is given by $\tau_1 = -a_1 R_B'/R_B^2$.

The second-order solution is found to be

$$\left.\begin{aligned} p_2 &= p_2 - \Omega\alpha_1^2 a_1 \int_0^{\tilde{y}} R_B U_B^2 \,\mathrm{d}\tilde{y},\\ v_2 &= \mathrm{i}\omega a_1 + \mathrm{i}\alpha_1 U_B\left[-a_2 + \Omega p_1 \int^{\tilde{y}} \left(\frac{1}{R_B U_B^2} - M^2\right)\mathrm{d}\tilde{y}\right],\\ u_2 &= -\frac{\alpha_2}{\alpha_1}a_1 U_B' - \frac{\Omega p_1}{R_B U_B} - U_B'\left[-a_2 + \Omega p_1 \int^{\tilde{y}} \left(\frac{1}{R_B U_B^2} - M^2\right)\mathrm{d}\tilde{y}\right],\\ \rho_2 &= -\frac{\alpha_2}{\alpha_1}a_1 R_B' + \Omega p_1 M^2 R_B - R_B'\left[-a_2 + \Omega p_1 \int^{\tilde{y}} \left(\frac{1}{R_B U_B^2} - M^2\right)\mathrm{d}\tilde{y}\right], \end{aligned}\right\} \tag{2.43}$$

while the second-order temperature τ_2 is related to ρ_2 via the relation

$$\tau_2 = \Omega\gamma M^2 p_1/R_B - \rho_2/R_B^2. \tag{2.44}$$

As $\tilde{y} \to \infty$,

$$\left.\begin{aligned} v_2 &\sim \Omega(\mathrm{i}\alpha_1 p_1)(1-M^2)\tilde{y} + (-\mathrm{i}\alpha_1 a_1 + \mathrm{i}\omega a_1 + \Omega \mathrm{i}\alpha_1 J_\infty p_1) + \cdots, \\ p_2 &\sim \left(-\Omega\alpha_1^2 a_1\right)\tilde{y} + \left(\tilde{p}_2 - \Omega\alpha_1^2 a_1 I_2\right) + \cdots. \end{aligned}\right\} \tag{2.45}$$

On other hand, as $\tilde{y} \to 0$,

$$u_2 \sim (\lambda_2/\lambda^2)p_1 \ln\tilde{y} + \left(\lambda a_2 - (\alpha_2/\alpha_1)\lambda a_1 - \Omega\lambda J_0 p_1 + \tfrac{3}{2}(\lambda_2/\lambda^2)p_1\right) + \cdots. \tag{2.46}$$

In the upper deck, the T-S wave solution expands as

$$(\boldsymbol{u}_I, p_I, \rho_I) = \delta\epsilon\{(\bar{\boldsymbol{u}}_1, \bar{p}_1, \bar{\rho}_1,) + \epsilon(\bar{\boldsymbol{u}}_2, \bar{p}_2, \bar{\rho}_2) + \cdots\}E + \text{c.c.} \tag{2.47}$$

The leading terms are governed by the equations

$$\bar{p}_{1,\bar{y}\bar{y}} - (1-M^2)\alpha^2\bar{p}_1 = 0, \quad \mathrm{i}\alpha_1\bar{\rho}_1 + \mathrm{i}\alpha_1\bar{u}_1 + \bar{v}_{1,\bar{y}} = 0, \quad \bar{u}_1 = -\bar{p}_1, \quad \mathrm{i}\alpha_1\bar{v}_1 = -\bar{p}_{1,\bar{y}},$$

which have the solution

$$(\bar{u}_2, \bar{v}_1, \bar{p}_1, \bar{\rho}_1) = \left(-1, -\mathrm{i}(1-M^2)^{1/2}, 1, M^2\right)p_1\,\mathrm{e}^{-\gamma_1\bar{y}}, \tag{2.48}$$

where $\gamma_1 = (1-M^2)^{1/2}\alpha_1$, and the constant p_1 is related to a_1 via

$$p_1 = \alpha_1/(1-M^2)^{1/2}a_1, \tag{2.49}$$

which follows from matching the leading-order vertical velocities in the upper and main decks.

The second-order terms in the expansion (2.47) are governed by the equations

$$\left.\begin{aligned} \bar{p}_{2,\bar{y}\bar{y}} - (1-M^2)\alpha_1^2\bar{p}_2 &= 2(1-M^2)\alpha_1\alpha_2\bar{p}_1 + 2M^2\omega\alpha_1\bar{p}_1, \\ \mathrm{i}\alpha_1\bar{v}_2 + \mathrm{i}(\alpha_2-\omega)\bar{v}_1 &= -\bar{p}_{2,\bar{y}}, \end{aligned}\right\} \tag{2.50}$$

which have the solution

$$\bar{p}_2 = \left\{\left(\tilde{p}_2 - \Omega\alpha_1^2 a_1 I_2\right) - (1-M^2)^{-1/2}qp_1\bar{y}\right\}\exp(-\gamma_1\bar{y}),$$

$$\bar{u}_2 = \left\{-\left(\tilde{p}_2 - \Omega\alpha_1^2 a_1 I_2\right) + (1-M^2)^{-1/2}q\bar{y} - (\omega/\alpha_1)p_1\right\}\exp(-\gamma_1\bar{y}),$$

$$\bar{v}_2 = \mathrm{i}(1-M^2)^{1/2}\left\{-\left(\tilde{p}_2 - \Omega\alpha_1^2 a_1 I_2\right) + (1-M^2)^{-1/2}qp_1\bar{y} - \frac{\omega/\alpha_1}{1-M^2}p_1\right\}\exp(-\gamma_1\bar{y}),$$

where we have put $q = (1-M^2)\alpha_2 + M^2\omega$, and use has been made of the matching condition for the pressure with the main deck. Matching the vertical velocities in the main and upper decks yields

$$-\mathrm{i}(1-M^2)^{1/2}\left\{\left(\tilde{p}_2 - \Omega\alpha_1^2 a_1 I_2\right) + \frac{\omega/\alpha_1}{1-M^2}p_1\right\} = -\mathrm{i}\alpha_1 a_2 + \mathrm{i}\omega a_1 + \Omega\mathrm{i}\alpha_1 p_1 J_\infty. \tag{2.51}$$

In the lower deck, the T-S wave solution expands as

$$\left.\begin{aligned} (u_I, v_I) &= \delta\Omega^{-1}\{(\tilde{u}_1, \epsilon^2\tilde{v}_1) + \epsilon(\tilde{u}_2, \epsilon^2\tilde{v}_2) + \cdots\}E + \text{c.c.}, \\ p_I &= \delta\epsilon\{p_1 + \epsilon\tilde{p}_2 + \cdots\}E + \text{c.c.}, \\ \rho_I &= \delta\epsilon\Omega^2\{\tilde{\rho}_1 + \epsilon\tilde{\rho}_2 + \cdots\}E + \text{c.c.} \end{aligned}\right\} \tag{2.52}$$

The leading-order T-S wave satisfies the linearized boundary-layer equations, on eliminating the pressure from which, it can be shown that $\tilde{u}_{1,Y}$ satisfies

$$\left\{\frac{\partial^2}{\partial Y^2} - \mathrm{i}(\alpha_1\lambda Y - \hat{\omega})\right\}\tilde{u}_{1,Y} = 0, \tag{2.53}$$

where $\hat{\omega} = \Omega\omega$. The solution satisfying the required no-slip condition is

$$\tilde{u}_1 = \int_{\eta_0}^{\eta} \mathrm{Ai}(\eta)\,\mathrm{d}\eta, \tag{2.54}$$

where Ai denotes the Airy function, and

$$\eta = (\mathrm{i}\alpha_1\lambda)^{1/3}Y + \eta_0, \quad \eta_0 = -\mathrm{i}\hat{\omega}(\mathrm{i}\alpha_1\lambda)^{-2/3}. \tag{2.55}$$

The no-slip condition $\tilde{u}_1(0) = \tilde{v}_1(0) = 0$ implies that $\tilde{u}_{1,YY}(0) = \mathrm{i}\alpha_1 p_1$. This and the matching requirement with the main-deck solution give rise to

$$(\mathrm{i}\alpha_1\lambda)^{2/3}\mathrm{Ai}'(\eta_0) = \mathrm{i}\alpha_1 p_1, \quad \int_{\eta_0}^{\infty} \mathrm{Ai}(\eta)\,\mathrm{d}\eta = \lambda a_1. \tag{2.56}$$

Elimination of p_1 and a_1 from (2.49) and (2.56) yields the dispersion relation (Smith 1989)

$$\Delta(\lambda) \equiv \int_{\eta_0}^{\infty} \mathrm{Ai}(\eta)\,\mathrm{d}\eta + \frac{\mathrm{i}\lambda}{\alpha_1^2}(1-M^2)^{\frac{1}{2}}(\mathrm{i}\alpha_1\lambda)^{2/3}\mathrm{Ai}'(\eta_0) = 0, \tag{2.57}$$

which determines α_1 for a given frequency ω.

It follows from the x-momentum equation that the leading-order transverse velocity of the T-S wave is given by

$$\tilde{v}_1 = \frac{1}{\lambda}\left\{\tilde{u}^{(1)}_{1,YY} - \mathrm{i}(\alpha_1\lambda Y - \hat{\omega})\tilde{u}_1 - \mathrm{i}\alpha_1 p_1\right\}. \tag{2.58}$$

Expansion of the linearized boundary-layer equation to the second order shows that $\tilde{u}_2$ satisfies

$$\left\{\frac{\partial^2}{\partial Y^2} - \mathrm{i}(\alpha_1\lambda Y - \hat{\omega})\right\}\tilde{u}_{2,Y} = \mathrm{i}\alpha_2\lambda Y\tilde{u}_{1,YY} + \tfrac{1}{2}\lambda_2(\mathrm{i}\alpha_1 Y^2\tilde{u}_{1,Y} + 2\tilde{v}_1), \tag{2.59}$$

subject to the usual homogeneous boundary condition $\tilde{u}_2 = \tilde{v}_2 = 0$; the latter is equivalent to $\tilde{u}_{2,YY}(0) = \mathrm{i}\alpha_1\tilde{p}_2 + \mathrm{i}\alpha_2 p_1$. The appropriate solution for the streamwise velocity is

$$\begin{aligned}\tilde{u}_2 = {} & \frac{\alpha_2}{\alpha_1}\left\{-\eta_0(\mathrm{Ai}(\eta) - \mathrm{Ai}(\eta_0)) + \tfrac{1}{3}(\eta\mathrm{Ai}(\eta) - \eta_0\mathrm{Ai}(\eta_0))\right\} \\ & + \tfrac{1}{2}(\lambda_2/\lambda)(\mathrm{i}\alpha_1\lambda)^{-1/3}\left\{\tfrac{1}{5}(\eta^2\mathrm{Ai}(\eta) - 3\mathrm{Ai}'(\eta)) - \tfrac{2}{3}\eta_0\eta\mathrm{Ai}(\eta) + \eta_0^2\mathrm{Ai}(\eta)\right. \\ & \left. + 2\int_{\eta_0}^{\eta}(\eta - \tilde{\eta})\mathrm{Ai}(\tilde{\eta})\,\mathrm{d}\tilde{\eta} - 2\mathrm{Ai}'(\eta_0)\int_{\eta_0}^{\eta} M(\tilde{\eta}, \eta_0)\,\mathrm{d}\tilde{\eta} - \tfrac{8}{15}\eta_0\mathrm{Ai}'(\eta_0) + \tfrac{13}{15}\mathrm{Ai}'(\eta_0)\right\} \\ & + q_2\int_{\eta_0}^{\eta}\mathrm{Ai}(\tilde{\eta})\,\mathrm{d}\tilde{\eta},\end{aligned} \tag{2.60}$$

where q_2 is an arbitrary constant, and $M(\eta, \eta_0)$ is defined by (2.38). The expansion of the x-momentum equation leads to the relation

$$\tilde{v}_2 = \lambda^{-1}\left\{\tilde{u}_{2,YY} - \mathrm{i}(\alpha_1\lambda Y - \hat{\omega})\tilde{u}_2 - \mathrm{i}\alpha_2\lambda Y\tilde{u}_1 - \mathrm{i}\alpha_1\tilde{p}_2 - \mathrm{i}\alpha_2 p_1 - \tfrac{1}{2}\lambda_2(Y^2\mathrm{i}\alpha_1\tilde{u}_1 + 2Y\tilde{v}_1)\right\}. \tag{2.61}$$

By applying the boundary condition and matching with the main-deck solution, we have

$$\left.\begin{aligned}&(\mathrm{i}\alpha_1\lambda)^{2/3}\left\{\frac{2}{3}\frac{\alpha_2}{\alpha_1}\left[\mathrm{Ai}'(\eta_0)-\eta_0^2\mathrm{Ai}(\eta_0)\right]+q_2\mathrm{Ai}'(\eta_0)\right\}+Q_0=\mathrm{i}\alpha_1\tilde{p}_2+\mathrm{i}\alpha_2 p_1,\\&\frac{2}{3}\frac{\alpha_2}{\alpha_1}\eta_0\mathrm{Ai}(\eta_0)+q_2\int_{\eta_0}^{\infty}\mathrm{Ai}(\eta)\,\mathrm{d}\eta+Q_\infty=\lambda a_2-\left(\frac{\alpha_2}{\alpha_1}\right)\lambda a-\Omega\lambda J_0 p_1+\tfrac{3}{2}\left(\frac{\lambda_2}{\lambda^2}\right)p_1,\end{aligned}\right\}\tag{2.62}$$

where we have put

$$\begin{aligned}Q_0&=\tfrac{1}{2}(\lambda_2/\lambda)(\mathrm{i}\alpha_1\lambda)^{1/3}\left\{\tfrac{8}{15}\eta_0^3\mathrm{Ai}(\eta_0)-\tfrac{17}{15}\eta_0\mathrm{Ai}'(\eta_0)+\tfrac{9}{5}\mathrm{Ai}(\eta_0)\right.\\&\qquad\left.+2\pi\mathrm{Ai}'(\eta_0)\mathrm{Bi}'(\eta_0)\int_{\eta_0}^{\infty}\mathrm{Ai}(\eta)\,\mathrm{d}\eta\right\},\\Q_\infty&=\tfrac{1}{2}(\lambda_2/\lambda)(\mathrm{i}\alpha_1\lambda)^{-1/3}\left\{-\tfrac{8}{15}\eta_0^2\mathrm{Ai}(\eta_0)-\tfrac{2}{5}\mathrm{Ai}'(\eta_0)\right.\\&\qquad\left.-2\mathrm{Ai}'(\eta_0)\left[\int_{\eta_0}^{\infty}\left(M(\eta,\eta_0)+\frac{1}{\eta}\right)\mathrm{d}\eta-\ln\Omega(\mathrm{i}\alpha_1\lambda)^{1/3}/(\epsilon\eta_0)\right]\right\}.\end{aligned}$$

It follows from (2.51) and (2.62) that

$$\begin{aligned}&\frac{\alpha_2}{\alpha_1}\left\{\tfrac{2}{3}\eta_0\mathrm{Ai}(\eta_0)+2\int_{\eta_0}^{\infty}\mathrm{Ai}(\eta)\,\mathrm{d}\eta+\frac{2}{3}\frac{\mathrm{i}\lambda(\mathrm{i}\alpha_1\lambda)^{2/3}(1-M^2)^{1/2}}{\alpha_1^2}\left(\mathrm{Ai}'(\eta_0)-\eta_0^2\mathrm{Ai}(\eta_0)\right)\right\}\\&\quad=\frac{\alpha_1}{(1-M^2)^{1/2}}\left\{\frac{(2-M^2)\omega}{\alpha_1^2(1-M^2)^{1/2}}+\Omega[J_\infty-J_0-(1-M^2)I_2]\right\}\int_{\eta_0}^{\infty}\mathrm{Ai}(\eta)\,\mathrm{d}\eta\\&\qquad-Q_\infty-\frac{\mathrm{i}(1-M^2)^{1/2}\lambda}{\alpha_1^2}Q_0,\end{aligned}\tag{2.63}$$

which determines α_2, the second-order correction to the dispersion relation.

3. The unsteady flow: scattering of T-S wave

In this section, we consider the scattered field. In physical space, its solution can be written as

$$(\tilde{\boldsymbol{u}}_s,\,\tilde{p}_s,\,\tilde{\rho}_s,\,\tilde{\tau}_s)=(\boldsymbol{u}_s,\,p_s,\,\rho_s,\,\tau_s)\,\mathrm{e}^{-\mathrm{i}\omega\bar{t}}+\mathrm{c.c.}\tag{3.1}$$

The governing equations for $(\boldsymbol{u}_s,\,p_s,\,\rho_s)$ are to be derived by substituting (3.1) and (2.16) into (2.9), (2.11) and (2.14)–(2.15). The solution for $(\boldsymbol{u}_s,\,p_s,\,\rho_s)$ is sought in each deck by taking a Fourier transform with respect to $\bar{x}$. The resulting flow quantities in the spectral space will be denoted by $(\widehat{\boldsymbol{u}}_s,\,\widehat{p}_s,\,\widehat{\rho}_s)$, respectively.

It turns out that the solution for this part of the unsteady motion must be obtained accurate up to $O(\epsilon^3)$ even for the purpose of determining the leading-order acoustic radiation in the far field. The reason is that two types of orderings are involved in the solution: the *asymptotic ordering* characterizing the near field hydrodynamic motion (i.e. the strength of the sources), and the *multipole ordering*, which reflects the radiating nature of the respective source.† The near-field solutions at the first four consecutive orders are such that they represent an octupole, quadrupole, dipole and monopole, respectively. The decreasing strength of the lower-order multipoles is

† The authors would like to thank a referee for suggesting the terminology used here.

exactly compensated by their increasing efficiency, with the consequence that they all make equal-order of magnitude contributions to the far-field sound.

The necessity of considering both the asymptotic and multipole orderings is due to the fundamental progress of sound radiation, namely, source cancellations. The first and primary cancellation occurs in the spectral space, among the radiating components, i.e. among the Fourier components with small wavenumbers. Usually, this kind of cancellation makes the asymptotic ordering disordered in the small-wavenumber limit. The second type of cancellation occurs in physical space, among the sources in different transverse regions. We shall point to these cancellations at the appropriate junctions of our analysis.

The algebra in this section is complicated, and we would like to direct the reader's attention to the main results, (3.61), (3.74), (3.78) and (3.80), from which the solution for the acoustic field can be obtained (§ 4).

3.1. *The main deck*

In the main deck, the Fourier transform of the scattered field has the expansion

$$\left.\begin{aligned}\widehat{u}_s &= \delta h \Omega^{-1}(U_1 + \epsilon U_2 + \epsilon^2 U_3 + \epsilon^3 U_4 + \cdots),\\ \widehat{v}_s &= \delta h \epsilon (V_1 + \epsilon V_2 + \epsilon^2 V_3 + \epsilon^3 V_4 + \cdots),\\ \widehat{p}_s &= \delta h \epsilon (P_1 + \epsilon P_2 + \epsilon^2 P_3 + \epsilon^3 P_4 + \cdots),\\ \widehat{\rho}_s &= \delta h \Omega^{-1}(R_1 + \epsilon R_2 + \epsilon^2 R_3 + \epsilon^3 R_4 + \cdots).\end{aligned}\right\} \tag{3.2}$$

The leading-order scattered field is induced by the dominant interaction between the T-S wave and the mean-flow distortion, which takes place in the lower deck because both concentrate in that region. The leading terms in the main-deck expansion (3.2) satisfy the familiar homogeneous main-deck equations, and have the solution

$$U_1 = A_1 U_B'(\tilde{y}), \quad V_1 = -\mathrm{i}k A_1 U_B, \quad R_1 = A_1 R_B'. \tag{3.3}$$

where A_1 is a function of k.

The terms U_2, V_2, etc. stand for the $O(R^{-1/8})$ correction to the scattered field. They satisfy the inhomogeneous equations

$$\left.\begin{aligned}\mathrm{i}k(R_B U_2 + U_B R_2) + (R_B V_2)_{\tilde{y}} &= \mathrm{i}\omega R_1 + \Omega^{-1} S_2,\\ R_B(\mathrm{i}k U_B U_2 + U_B' V_2) &= \mathrm{i}\omega R_B U_1 - \Omega \mathrm{i}k P_1 + \Omega^{-1} D_2,\\ \mathrm{i}k U_B R_2 + R_B' V_2 &= \mathrm{i}\omega R_1 + \Omega \mathrm{i}k P_1 M^2 R_B U_B + \Omega^{-1} E_2,\\ \mathrm{i}k\Omega R_B U_B V_1 &= -P_{2,\tilde{y}}.\end{aligned}\right\} \tag{3.4}$$

The forcing terms in (3.4) are given by

$$\left.\begin{aligned}S_2 &= -\left[\mathrm{i}k\left(u_1 R_m^{(1)} + \rho_1 U_m^{(1)}\right) + \left(v_1 R_m^{(1)} + \rho_1 V_m^{(1)}\right)_{\tilde{y}}\right],\\ D_2 &= -R_B\left[\mathrm{i}k u_1 U_m^{(1)} + v_1 U_{m,\tilde{y}}^{(1)} + u_{1,\tilde{y}} V_m^{(1)}\right],\\ E_2 &= R_B^2\left[\mathrm{i}\alpha\tau_1 U_m^{(1)} + \mathrm{i}(k-\alpha)u_1\tau_m^{(1)} + V_m^{(1)}\tau_{1,\tilde{y}} + v_1\tau_{m,y}\right]\\ &\quad - \mathrm{i}k R_B U_B\left(\rho_1\tau_m^{(1)} + \tau_1 R_m^{(1)}\right).\end{aligned}\right\} \tag{3.5}$$

They are contributed by the interaction between the T-S wave and mean-flow distortion. We remind the reader that the latter (corresponding to the quantities with the subscript m) are evaluated at $(k-\alpha)$. On eliminating R_2 from (3.4), it can be shown that

$$\mathrm{i}k U_2 + V_2' = -\mathrm{i}k\Omega M^2 U_B P_1 + \epsilon(-\mathrm{i}\alpha_2) a_1 A_m^{(1)}\left[2U_B R_B'^2/R_B^2 + R' U_B'/R_B\right], \tag{3.6}$$

$$R_B(U_B V_2' - U_B' V_2) = \mathrm{i}k P_1\left(1 - M^2 R_B U_B^2\right) - \mathrm{i}\omega R_B U_1 + \Omega^{-1} F_D^{(2)}, \tag{3.7}$$

where we have put

$$F_D^{(2)} = -\mathrm{i}ka_1 A_m^{(1)} R_B\left(U_B U_B'' - U_B'^2\right) + \epsilon \mathrm{i}\alpha_2 a_1 A_m^{(1)}\left(R_B U_B U_B'' - 2U_B^2 R_B'^2/R_B - U_B U_B' R_B'\right). \tag{3.8}$$

The $O(\epsilon)$ terms in (3.6) and (3.8) arise because α expands as (2.41). These terms must be handled carefully. They are in fact a dipole source, and it is convenient to relegate them to the next order, where all such contributions will be considered together. Note that the first two terms in (2.41) suffice, because the $O(\epsilon^2)$ correction, α_2, contributes at most a dipole which is weaker by a factor ϵ.

Equation (3.7) is solved to give

$$V_2 = -\mathrm{i}kA_2 U_B + \mathrm{i}\omega A_1 + \mathrm{i}kP_1 \Omega U_B \int^{\tilde{y}} \left(\frac{1}{R_B U_B^2} - M^2\right) \mathrm{d}\tilde{y} - \Omega^{-1}\mathrm{i}ka_1 A_m^{(1)} U_B'. \tag{3.9}$$

while (3.4) gives

$$P_2 = \tilde{P}_2 - \Omega k^2 A_1 \int_0^y R_B U_B^2 \,\mathrm{d}\tilde{y}, \tag{3.10}$$

where A_2 and $\tilde{P}_2$ are constants to be determined later. After inserting (3.9) into (3.6), it is found that

$$U_2 = A_2 U_B' - \Omega P_1 \left\{\frac{1}{R_B U_B} + U_B' \int^{\tilde{y}} \left(\frac{1}{R_B U_B^2} - M^2\right) \mathrm{d}\tilde{y}\right\} + \Omega^{-1} a_1 A_m^{(1)} U_B''. \tag{3.11}$$

It follows that as $\tilde{y} \to \infty$,

$$\left.\begin{aligned} V_2 &\sim \Omega(\mathrm{i}kP_1)(1-M^2)\tilde{y} + (-\mathrm{i}kA_2 + \mathrm{i}\omega A_1 + \Omega \mathrm{i}kP_1 J_\infty) + \cdots, \\ P_2 &\sim (-\Omega k^2 A_1)\tilde{y} + (\tilde{P}_2 - \Omega k^2 A_1 I_2) + \cdots, \end{aligned}\right\} \tag{3.12}$$

where J_∞ and I_2 are defined by (A 4), and (A 1), respectively. On the other hand, as $\tilde{y} \to 0$,

$$U_2 \sim (\lambda_2/\lambda^2) P_1 \ln \tilde{y} + \left(\lambda A_2 - \Omega \lambda J_0 P_1 + \tfrac{3}{2}(\lambda_2/\lambda^2) P_1 + \lambda_2 a_1 A_m^{(1)}\right).$$

The term $\lambda_2 a_1 A_m^{(1)}$ represents the net contribution from the forcing term (the quadrupole source) in the main deck. This contribution is zero for the Blasius boundary layer, for which $\lambda_2 = 0$. This observation testifies to the basic fact that the relevant acoustic source is intrinsically dependent on the background base flow. The influence of the latter on the sound wave cannot be fully characterized in terms of refraction or 'flow shielding'.

The governing equations for $(U_3,\ V_3,\ R_3,\ P_3)$ are

$$\mathrm{i}k(R_B U_3 + U_2 R_3) + (R_B V_3)_{\tilde{y}} = \mathrm{i}\omega R_2 + \Omega^{-1} S_3, \tag{3.13a}$$

$$R_B(\mathrm{i}kU_B U_3 + U_B' V_3) = \mathrm{i}\omega R_B U_2 - \Omega \mathrm{i}kP_2 + \Omega^{-1} D_3, \tag{3.13b}$$

$$\mathrm{i}kU_B R_3 + R_B' V_3 = \mathrm{i}\omega R_2 + \Omega M^2 R_B(\mathrm{i}kP_2 U_B - \mathrm{i}\omega P_1) + \Omega^{-1} E_3, \tag{3.13c}$$

$$\Omega R_B(-\mathrm{i}\omega V_1 + \mathrm{i}kU_B V_2) = -P_{3,\tilde{y}} + G_3, \tag{3.13d}$$

where the forcing terms S_3, D_3, E_3 and G_3 are given by (A 6)–(A 9) in the Appendix. Again, we eliminate R_3, U_3 to obtain the equation for V_3:

$$R_B(U_B V_3' - U_B' V_3) = \mathrm{i}kP_2\left(1 - M^2 R_B U_B^2\right) - \mathrm{i}\omega R_B U_2 + \Omega^{-1} F_D^{(3)}. \tag{3.14}$$

The exact expression for $F_D^{(3)}$ is lengthy. Fortunately, at the present order we need only consider the dipole source, corresponding to which $P_3 \sim O(k^0)$ for $k \ll 1$. The

terms proportional to k (or higher powers) are omitted since they represent a source of quadrupole (or high-order poles), whose contribution is much smaller. Then $F_D^{(3)}$ reduces to

$$F_D^{(3)} = \Omega \mathrm{i}\alpha\big(p_1 A_m^{(1)} - a_1 P_m^{(1)}\big)\big\{(\gamma-1)M^2\big(U_B^2 R_B' - R_B U_B U_B'\big) + R'/R_B\big\} + \mathrm{i}\omega a_1 A_m^{(1)} R_B U_B'' - \mathrm{i}\alpha_2 a_1 A_m^{(1)}\big\{R_B U_B U_B'' - 2U_B^2 R_B'^2/R_B - U_B U_B' R_B'\big\} + \{\text{terms} \sim k\}, \tag{3.15}$$

in which the terms proportional to α_2 cancel out the $O(\epsilon)$ term in (3.8) that is relegated to the present order. It must be pointed out that inclusion (exclusion) of relevant (irrelevant) terms is not an *ad hoc* assertion; rather, it is strictly based on the acoustic nature of the terms concerned, which can be identified by examining their small-k behaviour.

From (3.14) and (3.13*a*), we have

$$\begin{aligned} V_3 = {} & -\mathrm{i}kA_3 U_B + \mathrm{i}\omega A_2 + \Omega(\mathrm{i}k\tilde{P}_2)U_B \int^{\tilde{y}} \left(\frac{1}{R_B U_B^2} - M^2\right) \mathrm{d}\tilde{y} \\ & - \Omega^2(\mathrm{i}k^3)A_1 U_B \int_0^{\tilde{y}} \left(\frac{1}{R_B U_B^2} - M^2\right) \int_0^{\tilde{y}} R_B U_B^2 \,\mathrm{d}\tilde{y} \\ & + \Omega(\mathrm{i}\omega P_1)U_B \left\{2\int^{\tilde{y}} \frac{1}{R_B U_B^3}\,\mathrm{d}\tilde{y} - \frac{1}{U_B}\int^{\tilde{y}} \left(\frac{1}{R_B U_B^2} - M^2\right)\mathrm{d}\tilde{y}\right\} \\ & + \mathrm{i}\alpha\big(p_1 A_m^{(1)} - a_1 P_m^{(1)}\big)U_B \int_\infty^{\tilde{y}} \left\{(\gamma-1)M^2\left(\frac{R_B'}{R_B} - \frac{U_B'}{U_B}\right) + \frac{R_B'}{R_B^2 U_B^2}\right\} \mathrm{d}\tilde{y}, \end{aligned} \tag{3.16}$$

$$\begin{aligned} P_3 = {} & \tilde{P}_3 + \Omega\left\{2\omega k A_1 \int_0^{\tilde{y}} R_B U_B \,\mathrm{d}\tilde{y} - k^2 A_2 \int_0^{\tilde{y}} R_B U_B^2 \,\mathrm{d}\tilde{y}\right. \\ & \left. + \Omega k^2 P_1 \int_0^{\tilde{y}} R_B U_B^2 \int^{y} \left(\frac{1}{R_0 U_B^2} - M^2\right)\mathrm{d}\tilde{y}\right\} \\ & - a_1 A_m^{(1)}\left\{\tfrac{1}{2}(2\alpha - k)^2 R_B U_B^2 + \tfrac{1}{2}k^2 \int_0^{\tilde{y}} R_B' U_B^2 \,\mathrm{d}\tilde{y}\right\}, \end{aligned} \tag{3.17}$$

where A_3 and $\tilde{P}_3$ are functions of k to be found. It can be shown that as $\tilde{y} \to \infty$,

$$\begin{aligned} V_3 \sim {} & -\tfrac{1}{2}(1-M^2)\Omega^2 \mathrm{i}k A_1 \tilde{y}^2 + \{-\Omega^2 \mathrm{i}k^3(1-M^2)I_2 A_1 + \Omega\mathrm{i}\omega(1+M^2)P_1\}\tilde{y} \\ & + \{-\mathrm{i}kA_3 + \mathrm{i}\omega A_2 + \{O(k^2)\text{ terms}\}\} + \cdots, \end{aligned} \tag{3.18}$$

$$\begin{aligned} P_3 \sim {} & \tfrac{1}{2}(1-M^2)\Omega^2 k^2 P_1 \tilde{y}^2 + \Omega\{2\omega k A_1 - k^2 A_2 + \Omega k^2 P_1 J_\infty\}\tilde{y} \\ & + \big\{\tilde{P}_3 - 2\alpha^2 a_1 A_m^{(1)} + \{O(k^2)\text{ terms}\}\big\} + \cdots. \end{aligned} \tag{3.19}$$

Elimination of R_3 in (3.13*a*)–(3.13*c*) yields

$$\begin{aligned} \mathrm{i}kU_3 + V_3' = {} & -\Omega M^2 \mathrm{i}k P_2 U_B + \Omega M^2 \mathrm{i}\omega P_1 \\ & + \mathrm{i}\alpha M^2\big(a_1 P_m^{(1)} - p_1 A_m^{(1)}\big)\{\gamma(U_B' - U_B R_B'/R_B) + R_B' U_B/R_B\}, \end{aligned} \tag{3.20}$$

from which it can be deduced that as $\tilde{y} \to 0$,

$$U_3 \sim 2\Omega(\gamma-1)M^2\left(\frac{\omega P_1}{k}\right)\ln\tilde{y} + \lambda A_3 + (\alpha/k)\big(a_1 P_m^{(1)} - p_1 A_m^{(1)}\big)\lambda I_M + \{O(k)\text{ terms}\}, \tag{3.21}$$

where I_M is defined by (A 2) in the Appendix.

Finally, consider (U_4, V_4, P_4). At this order of approximation, the relevant source is a monopole, corresponding to which $P_4 \sim O(k^{-1})$ for $k \ll 1$. We can ignore all the

terms representing sources of dipole, quadrupole, etc., at this order. These include the interaction between the T-S wave and mean-flow distortion at the present order, which contributes a dipole at most. On inspecting the small-k limit of the inhomogeneous term, and retaining only the terms contributing to a monopole, the governing equation for V_4 simply reads

$$U_B V_4' - U_B' V_4 = -\mathrm{i}\omega U_3 + \cdots. \tag{3.22}$$

The relevant part of the full solution is

$$\begin{aligned} V_4 = {} & -\mathrm{i}kA_4 U_B + \mathrm{i}\omega A_3 - \mathrm{i}\omega(\alpha/k)\big(a_1 P_m^{(1)} - p_1 A_m^{(1)}\big) \\ & \times \left\{ -M^2 - \int_\infty^{\tilde{y}} \left\{ (\gamma-1)M^2 \left(\frac{R_B'}{R_B} - \frac{U_B'}{U_B} \right) + \frac{R_B'}{R_B^2 U_B^2} \right\} \mathrm{d}\tilde{y} \right. \\ & \left. + U_B \int_\infty^{\tilde{y}} \left\{ (\gamma-1)M^2 \left(\frac{R_B'}{R_B U_B} - \frac{U_B'}{U_B^2} \right) + \frac{2R_B'}{R_B^2 U_B^3} \right\} \mathrm{d}\tilde{y} \right\}. \end{aligned} \tag{3.23}$$

It can be shown that as $\tilde{y} \to \infty$,

$$V_4 \sim -\mathrm{i}kA_4 + \mathrm{i}\omega\big[A_3 + (\alpha/k)M^2\big(a_1 P_m^{(1)} - p_1 A_m^{(1)}\big)\big]. \tag{3.24}$$

From the expansion of the continuity and energy equations, it can be deduced that as $\tilde{y} \to 0$,

$$U_4 \sim \lambda A_4 - (\omega\alpha/k^2)\big(a_1 P_m^{(1)} - p_1 A_m^{(1)}\big)\lambda J_M, \tag{3.25}$$

with J_M being given by (A 5).

3.2. *The upper-deck solution*

In the upper deck, it is convenient and informative to work with the pressure field $\tilde{p}_s = (p_s\,\mathrm{e}^{-\mathrm{i}\omega\bar{t}} + c.c.)$. In physical space, $\tilde{p}_s$ satisfies the inhomogeneous convected wave equation

$$M^2\left(\frac{\partial}{\partial t} + \frac{\partial}{\partial x}\right)^2 \tilde{p}_s - \nabla^2 \tilde{p}_s = R_p, \tag{3.26}$$

where

$$\begin{aligned} R_p = {} & \nabla\cdot\{(\tilde{\boldsymbol{u}}_m\cdot\nabla)\,\boldsymbol{u}_I + (\boldsymbol{u}_I\cdot\nabla)\tilde{\boldsymbol{u}}_m - \rho_m\nabla p_I - \rho_I\nabla p_m\} \\ & + (\tilde{\boldsymbol{u}}_m\cdot\nabla)(\nabla\cdot\boldsymbol{u}_I) + (\boldsymbol{u}_I\cdot\nabla)(\nabla\cdot\tilde{\boldsymbol{u}}_m) + 2M^2\nabla p_m\cdot\nabla p_I \\ & + 2\gamma(\nabla\cdot\tilde{\boldsymbol{u}}_m)(\nabla\cdot u_I) + \gamma M^2(p_m\nabla^2 p_I + p_I\nabla^2 p_m); \end{aligned} \tag{3.27}$$

here the subscripts I and m signify the flow quantities associated with the incident T-S wave and the mean-flow distortion, respectively. The velocity field of the scattered field, $\tilde{\boldsymbol{u}}_s = (\boldsymbol{u}_s\,\mathrm{e}^{-\mathrm{i}\omega\bar{t}} + \mathrm{c.c.})$, is related to the pressure gradient via the momentum equations

$$\left(\frac{\partial}{\partial t} + \frac{\partial}{\partial x}\right)\tilde{\boldsymbol{u}}_s = -\nabla p_s + \mathbf{R}_v, \tag{3.28}$$

where

$$\mathbf{R}_v = -(\tilde{\boldsymbol{u}}_m\cdot\nabla)\,\boldsymbol{u}_I - (\boldsymbol{u}_I\cdot\nabla)\tilde{\boldsymbol{u}}_m + \rho_m\nabla p_I + \rho_I\nabla p_m. \tag{3.29}$$

In the upper deck, it suffices to consider p_s and v_s only, whose Fourier transforms, $(\hat{v}_s,\ \hat{p}_s)$, can be written as

$$(\hat{v}_s,\ \hat{p}_s) = \delta h\epsilon\{(\hat{v}_1, \hat{p}_1) + \epsilon(\hat{v}_2, \hat{p}_2) + \epsilon^2(\hat{v}_3, \hat{p}_3) + \epsilon^3(\hat{v}_4, \hat{p}_4) + \cdots\}. \tag{3.30}$$

The governing equations for $\widehat{p}_1$ and $\widehat{v}_1$ are

$$\left\{\frac{\partial^2}{\partial\bar{y}^2}-(1-M^2)k^2\right\}\widehat{p}_1=0,\quad \mathrm{i}k\widehat{v}_1=-\widehat{p}_{1,\bar{y}}. \tag{3.31}$$

The solutions are

$$\widehat{p}_1=P_1\,\mathrm{e}^{-\bar{\kappa}\bar{y}},\quad \widehat{v}_1=\frac{\bar{\kappa}}{\mathrm{i}k}P_1\,\mathrm{e}^{-\bar{\kappa}\bar{y}}. \tag{3.32}$$

where $\bar{\kappa}=(1-M^2)^{1/2}|k|$. Matching $\bar{v}_1$ with the main-deck solution (3.3) gives

$$P_1=k^2/\bar{\kappa}A_1. \tag{3.33}$$

The governing equations for $\widehat{p}_2$ and $\widehat{v}_2$ in (3.30) are

$$\left\{\frac{\partial^2}{\partial\bar{y}^2}-(1-M^2)k^2\right\}\widehat{p}_2=2M^2\omega k\widehat{p}_1,\quad \mathrm{i}k\widehat{v}_2-\mathrm{i}\omega\widehat{v}_1=-\widehat{p}_{2,\bar{y}}. \tag{3.34}$$

We find that

$$\widehat{p}_2=\bar{P}_2\,\mathrm{e}^{-\bar{\kappa}\bar{y}}-\frac{M^2\omega k}{\bar{\kappa}}P_1\bar{y}\,\mathrm{e}^{-\bar{\kappa}\bar{y}}, \tag{3.35}$$

where $\bar{P}_2$ is an arbitrary function of k. Substituting $\widehat{p}_2$ into the equation for $\widehat{v}_2$, we find that as $\bar{y}\to 0$,

$$\widehat{v}_2\to\frac{\bar{\kappa}}{\mathrm{i}k}\bar{P}_2-\frac{\mathrm{i}\omega}{\bar{\kappa}}P_1. \tag{3.36}$$

The matching requirement for the pressure and vertical velocity with their main-deck counterparts leads to

$$\bar{P}_2=\tilde{P}_2-\Omega k^2A_1I_2,\quad \frac{\bar{\kappa}}{\mathrm{i}k}\bar{P}_2-\frac{\mathrm{i}\omega}{\bar{\kappa}}P_1=-\mathrm{i}kA_2+\mathrm{i}\omega A_1+\Omega(\mathrm{i}kP_1)J_\infty. \tag{3.37}$$

The functions $\widehat{p}_3$ and $\widehat{v}_3$ satisfy

$$\left.\begin{gathered}\left\{\frac{\partial^2}{\partial\bar{y}^2}-(1-M^2)k^2\right\}\widehat{p}_3=2M^2\omega k\widehat{p}_2-M^2\omega^2\widehat{p}_1+R_{3,p}\exp(-\bar{\kappa}_p\,\bar{y}),\\ \mathrm{i}k\widehat{v}_3-\mathrm{i}\omega\widehat{v}_2=-\widehat{p}_{3,\bar{y}}+R_{3,v}\exp(-\bar{\kappa}_p\,\bar{y}),\end{gathered}\right\} \tag{3.38}$$

where we have put $\bar{\kappa}_p=(1-M^2)^{1/2}(\alpha_1+\mu)$ with $\mu=|k-\alpha|$. $R_{3,p}$ and $R_{3,v}$ are the forcing due to the T-S wave interacting with the mean-flow distortion in the upper deck,

$$\begin{aligned}R_{3,p}=&-\left\{(1-M^2)^2[\alpha_1+\mu(k-\alpha)]^2\left(1-\frac{\mu}{k-\alpha}\right)+\epsilon(1-M^2)(\alpha_1+\mu)\alpha_2\right.\\&-(1-M^2)\left(1-\frac{\mu}{k-\alpha}\right)k^2-\gamma M^4k^2-M^2\left[1-\frac{(1-M^2)\mu}{k-\alpha}\right]k^2\\&\left.-\epsilon(1-M^2)\left[2\gamma M^2k+\left(1-\frac{\mu}{k-\alpha}\right)\alpha+\frac{2M^2\mu k}{k-\alpha}\right]\alpha_2\right\}p_1P_m^{(1)},\end{aligned} \tag{3.39}$$

$$R_{3,v}=\left\{(1-M^2)^{3/2}[\alpha_1+\mu(k-\alpha)]\left(1-\frac{\mu}{k-\alpha}\right)+\epsilon(1-M^2)^{1/2}\alpha_2\right\}p_1P_m^{(1)}. \tag{3.40}$$

In the above expressions, the $O(\epsilon)$ terms proportional to α_2 correspond to a monopole source, and they are relegated to the next order. The solution for $\widehat{p}_3$ is found

to be

$$\widehat{p}_3 = \bar{P}_3 \exp(-\bar{\kappa}\,\bar{y}) + \frac{M^4\omega^2}{2(1-M^2)} P_1 \bar{y}^2 \exp(-\bar{\kappa}\,\bar{y}) + \left\{ \frac{M^2\omega^2 P_1}{2(1-M^2)\bar{\kappa}} - \frac{M^2\omega k \bar{P}_2}{\bar{\kappa}} \right\} \bar{y} \exp(-\bar{\kappa}\,\bar{y}) + F_{3,p} \exp(-\bar{\kappa}_p \bar{y}), \tag{3.41}$$

where

$$F_{3,p} = (1-M^2)\frac{(\alpha_1+\mu)^2}{k^2-(\alpha_1+\mu)^2}\left(1-\frac{\mu}{k-\alpha}\right) p_1 P_m^{(1)}. \tag{3.42}$$

It follows from (3.38) that as $\bar{y} \to 0$,

$$\bar{v}_3 \to \frac{\bar{\kappa}}{\mathrm{i}k}\bar{P}_3 - \frac{\mathrm{i}\omega}{\bar{\kappa}}\bar{P}_2 - \frac{\mathrm{i}\omega^2 P_1}{\bar{\kappa}k}\left[1-\frac{M^2}{2(1-M^2)}\right] + F_{3,v}, \tag{3.43}$$

where

$$F_{3,v} = -(1-M^2)^{3/2}\frac{\mathrm{i}k(\alpha_1+\mu)}{k^2-(\alpha_1+\mu)^2}\left(1-\frac{\mu}{k-\alpha}\right) p_1 P_m^{(1)}.$$

Matching the pressure $\widehat{p}_3$ and the vertical velocity $\widehat{v}_3$ with their respective counterparts in the main deck yields

$$\bar{P}_3 + F_{3,p} = \tilde{P}_3 - 2\alpha^2 a_1 A_m^{(1)}, \tag{3.44a}$$

$$\frac{\bar{\kappa}}{\mathrm{i}k}\bar{P}_3 - \frac{\mathrm{i}\omega}{\bar{\kappa}}\bar{P}_2 - \frac{\mathrm{i}\omega^2 P_1}{\bar{\kappa}k}\left[1-\frac{M^2}{2(1-M^2)}\right] + F_{3,v} = -\mathrm{i}kA_3 + \mathrm{i}\omega A_2. \tag{3.44b}$$

Here, we neglected terms of $O(k)$ or smaller. Since $F_{3,v} \sim k$, its contribution is a quadrupole and will be ignored hereinafter. In (3.44*a*), $F_{3,p}$ and $-2\alpha^2 a_1 A_m^{(1)}$ represent the dipole contributions from the upper and main decks, respectively. Interestingly, they cancel each other. This represents a source cancellation in physical space. It suggests that the acoustic field depends on the source over a rather extensive region; merely prescribing sources within the boundary layer would not guarantee a correct prediction of the radiated sound.

The functions $\widehat{p}_4$ and $\widehat{v}_4$ satisfy

$$\left.\begin{aligned} \left\{\frac{\partial^2}{\partial\bar{y}^2} - (1-M^2)k^2\right\}\widehat{p}_4 &= 2M^2\omega k\widehat{p}_3 - M^2\omega^2\widehat{p}_2 + R_{4,p}\,\exp(-\bar{\kappa}_p\,\bar{y}), \\ \mathrm{i}k\widehat{v}_4 - \mathrm{i}\omega\widehat{v}_3 &= -\widehat{p}_{4,\bar{y}} + R_{4,v}\,\exp(-\bar{\kappa}_p\,\bar{y}), \end{aligned}\right\} \tag{3.45}$$

where $R_{4,p}$ and $R_{4,v}$ are given in the Appendix by (A 10) and (A 11), respectively. In these expressions, the terms proportional to k^2 and k represent quadrupole and dipole sources, and they are therefore negligible compared with the monopole source that we are seeking. With these terms being discarded, but taking into account the terms relegated from the previous order (i.e. the terms proportional to α_2 in (3.39) and (3.40)), it is found that

$$\widehat{p}_4 = \bar{P}_4 \exp(-\bar{\kappa}\,\bar{y}) - \frac{1}{6}\frac{M^6\omega^3 k P_1}{(1-M^2)\bar{\kappa}}\bar{y}^3 \exp(-\bar{\kappa}\,\bar{y}) + \frac{1}{2}\frac{M^4\omega^2}{1-M^2}\left(\bar{P}_2 - \frac{\omega P_1}{(1-M^2)k}\right)\bar{y}^2 \times \exp(-\bar{\kappa}\,\bar{y}) + \left\{-\frac{M^4\omega^3 P_1}{2(1-M^2)^2 k\bar{\kappa}} + \frac{M^2\omega^2\bar{P}_2}{2(1-M^2)\bar{\kappa}} - \frac{M^2\omega k\bar{P}_3}{\bar{\kappa}}\right\}\bar{y}\exp(-\bar{\kappa}\,\bar{y}) + (G_p\bar{y} + F_{4,p})\exp(-\bar{\kappa}_p\,\bar{y}), \tag{3.46}$$

where

$$G_p = (1-M^2)^{1/2}\frac{(\alpha_1+\mu)q}{k^2-(\alpha_1+\mu)^2}(k-2\alpha)\left[1-\frac{\mu}{k-\alpha}\right]p_1 P_m^{(1)},$$

$$F_{4,p} = \frac{1}{k^2-(\alpha_1+\mu)^2}\left\{(\alpha_1+\mu)[q-(k-2\alpha)\omega/\alpha_1]-\frac{k^2+(\alpha_1+\mu)^2}{k^2-(\alpha_1+\mu)^2}q(k-2\alpha)\right\}\left[1-\frac{\mu}{k-\alpha}\right]p_1 P_m^{(1)}.$$

By inserting $\widehat{p}_4$ into the momentum equation in (3.45), we can find the asymptote of $\widehat{v}_4$ as $\bar{y}\to 0$. Matching it with the main-deck solution gives

$$\frac{\bar{\kappa}}{\mathrm{i}k}\bar{P}_4 - \frac{\mathrm{i}\omega}{\bar{\kappa}}\bar{P}_3 - \frac{\mathrm{i}\omega^2\bar{P}_2}{\bar{\kappa}k}\left[1-\frac{M^2}{2(1-M^2)}\right] - \frac{\mathrm{i}\omega^3 P_1}{\bar{\kappa}k^2}\left[1-\frac{M^2(1-2M^2)}{2(1-M^2)^2}\right] + F_{4,v} = -\mathrm{i}kA_4 + \mathrm{i}\omega A_3 + \cdots, \tag{3.47}$$

while matching of the pressure leads to

$$\bar{P}_4 + F_{4,p} = \tilde{P}_4 + \cdots, \tag{3.48}$$

where

$$F_{4,v} = \frac{\mathrm{i}(1-M^2)^{1/2}}{k^2-(\alpha_1+\mu)^2}\left\{\frac{2q(\alpha_1+\mu)(k-2\alpha)}{k^2-(\alpha_1+\mu)^2} - [q-(k-2\alpha)\omega/\alpha_1]\right\}\left[1-\frac{\mu}{k-\alpha}\right]kp_1 P_m^{(1)}.$$

The contribution of the interaction between the T-S wave and mean-flow distortion in the upper deck is represented by $F_{4,p}$ and $F_{4,v}$. It is noted that $F_{4,p}\sim O(k^0)$ for $k\ll 1$, and through the vertical momentum equation in (3.45), we may expect that $F_{4,v}\sim O(k^{-1})$. However, our calculation shows that $F_{4,v}\sim O(k)$ owing to cancellation in the small -k limit between the two terms on the right-hand-side of (3.45). As a result, the contribution from the direct interaction in the upper deck at this order turns out to be negligible.

3.3. *The lower-deck solution*

In the lower deck, the Fourier transform of (u_s, v_s, p_s, ρ_s) has the expansion

$$\left.\begin{aligned}
\widehat{u}_s &= \delta h\Omega^{-1}(\tilde{U}_1+\epsilon\tilde{U}_2+\epsilon^2\tilde{U}_3+\epsilon^3\tilde{U}_4+\cdots\},\\
\widehat{v}_s &= \delta h\epsilon^2\Omega^{-1}(\tilde{V}_1+\epsilon\tilde{V}_2+\epsilon^2\tilde{V}_3+\epsilon^3\tilde{U}_4+\cdots),\\
\widehat{p}_s &= \delta h\epsilon(P_1+\epsilon\tilde{P}_2+\epsilon^2\tilde{P}_3+\epsilon^3\tilde{P}_4+\cdots),\\
\widehat{\rho}_s &= \delta h\epsilon\Omega^2(\tilde{R}_1+\epsilon\tilde{R}_2+\epsilon^2\tilde{R}_3+\epsilon^3\tilde{R}_4+\cdots).
\end{aligned}\right\} \tag{3.49}$$

The leading-order terms satisfy the linearized boundary-layer equations

$$\mathrm{i}k\tilde{U}_1 + \tilde{V}_{1,Y} = 0, \tag{3.50}$$

$$\mathrm{i}(k\lambda Y-\hat{\omega})\tilde{U}_1 + \lambda\tilde{V}_1 = -\mathrm{i}kP_1 + \tilde{U}_{1,YY} + N_1, \tag{3.51}$$

where we put

$$N_1 = -\mathrm{i}k\tilde{u}_1\tilde{U}_m^{(1)} - \tilde{V}_m^{(1)}\tilde{u}_{1,Y} - \tilde{v}_1\tilde{U}_{m,Y}^{(1)}. \tag{3.52}$$

Recall that the mean-flow quantities (i.e. those with the subscript m) are evaluated at $(k-\alpha)$. The system (3.50)–(3.51) is subject to the matching condition with the main deck:

$$\tilde{U}_1 \to \lambda A_1 \quad \text{as} \quad Y\to\infty. \tag{3.53}$$

The no-slip condition for the unsteady flow on $Y = hF_w(\bar{x})$ leads, after linearization for small h, to $\tilde{U}_1 = -\tilde{u}_{1,Y}(0)\widehat{F}$ and $\tilde{V}_1 = 0$ at $Y = 0$, which in turn imply that

$$\tilde{U}_1 = -\tilde{u}_{1,Y}(0)\widehat{F}, \quad \tilde{U}_{1,YY}(0) = \mathrm{i}\hat{\omega}\tilde{u}_{1,Y}(0)\widehat{F} + \mathrm{i}kP_1 \tag{3.54}$$

after setting $Y = 0$ in (3.51) and using the fact that $N_1 = 0$ at $Y = 0$.

By eliminating the pressure from (3.50)–(3.51), it can be shown that $\tilde{U}_1$ satisfies

$$\mathscr{L}\tilde{U}_{1,Y} \equiv \left\{\frac{\partial^2}{\partial Y^2} - \mathrm{i}(k\lambda Y - \hat{\omega})\right\}\tilde{U}_{1,Y} = (\mathrm{i}k\lambda)H_1, \tag{3.55}$$

where $H_1 \equiv -(\mathrm{i}k\lambda)^{-1}N_{1,Y}$ or more explicitly

$$\begin{aligned} H_1 = \frac{1}{\lambda}(\mathrm{i}k\lambda)^{-1}\big\{&\mathrm{i}(k-\alpha_1)\lambda\tilde{u}_1\tilde{U}^{(1)}_{m,Y} + \mathrm{i}\alpha\lambda\tilde{u}_{1,Y}\tilde{U}^{(1)}_m \\ &+ \tilde{u}_{1,YY}\big[\tilde{U}^{(1)}_{m,YY} - \mathrm{i}(k-\alpha)\lambda Y\tilde{U}^{(1)}_m - \mathrm{i}(k-\alpha)P^{(1)}_m\big] \\ &+ \tilde{U}^{(1)}_{m,YY}\big[\tilde{u}_{1,YY} - \mathrm{i}(\alpha_1\lambda Y - \hat{\omega})\tilde{u}_1 - \mathrm{i}\alpha_1 p_1\big]\big\}. \end{aligned} \tag{3.56}$$

Note that H_1 decays exponentially as $Y \to \infty$. The solution to (3.55) can be expressed as (cf. Goldstein 1985)

$$\tilde{U}_1 = -\tilde{u}_{1,Y}(0)\widehat{F} + \int_{\zeta_0}^{\zeta}\tilde{M}_1(\zeta,\zeta_0)\,\mathrm{d}\zeta + C_1(k)\int_{\zeta_0}^{\zeta}\mathrm{Ai}(\zeta)\,\mathrm{d}\zeta, \tag{3.57}$$

where

$$\tilde{M}_1(\zeta,\zeta_0) = \pi\left\{\mathrm{Bi}(\zeta)\int_{\infty}^{\zeta}\mathrm{Ai}(\tilde{\zeta})H_1(\tilde{Y})\,\mathrm{d}\tilde{\zeta} - \mathrm{Ai}(\zeta)\int_{\zeta_0}^{\zeta}\mathrm{Bi}(\tilde{\zeta})H_1(\tilde{Y})\,\mathrm{d}\tilde{\zeta}\right\}, \tag{3.58}$$

with Ai and Bi denoting the Airy functions, and

$$\zeta = (\mathrm{i}k\lambda)^{1/3}Y + \zeta_0, \quad \zeta_0 = -\mathrm{i}\hat{\omega}(\mathrm{i}k\lambda)^{-2/3}. \tag{3.59}$$

Application of the matching and boundary conditions, (3.53) and (3.54), gives

$$\left.\begin{aligned} -\tilde{u}_{1,Y}(0)\widehat{F} + \int_{\zeta_0}^{\infty}\tilde{M}_1(\zeta,\zeta_0)\,\mathrm{d}\zeta + C_1(k)\int_{\zeta_0}^{\infty}\mathrm{Ai}(\zeta)\,\mathrm{d}\zeta &= \lambda A_1, \\ (\mathrm{i}k\lambda)^{2/3}\left\{\pi\mathrm{Bi}'(\zeta_0)\int_{\infty}^{\zeta_0}\mathrm{Ai}(\zeta)H_1(Y)\,\mathrm{d}\zeta + C_1(k)\mathrm{Ai}'(\zeta_0)\right\} &= \mathrm{i}\hat{\omega}\tilde{u}_{1,Y}(0)\widehat{F} + \mathrm{i}kP_1. \end{aligned}\right\} \tag{3.60}$$

Eliminating A_1 and $C_1(k)$ from (3.33) and (3.60), we obtain

$$P_1 = -\frac{\mathrm{i}(\mathrm{i}k\lambda)^{2/3}\mathrm{Ai}'(\zeta_0)}{k\Delta(k;\hat{\omega})}\left\{\tilde{u}_{1,Y}(0)\widehat{F}(1+\zeta_0\mathscr{R}(\zeta_0)) + \int_{\zeta_0}^{\infty}K(\zeta,\zeta_0)H_1(Y)\,\mathrm{d}\zeta\right\}, \tag{3.61}$$

where

$$\Delta(k;\hat{\omega}) = \int_{\zeta_0}^{\infty}\mathrm{Ai}(\zeta)\,\mathrm{d}\zeta + \mathrm{i}\lambda(\mathrm{i}k\lambda)^{2/3}\mathrm{Ai}'(\zeta_0)\frac{\bar{\kappa}}{k^3}, \tag{3.62}$$

$$K(\zeta,\zeta_0) = \pi\frac{\mathrm{Ai}'(\zeta_0)\mathrm{Gi}(\zeta) - \mathrm{Gi}'(\zeta_0)\mathrm{Ai}(\zeta)}{\mathrm{Ai}'(\zeta_0)}, \tag{3.63}$$

$$\mathscr{R}(\zeta_0) = \int_{\zeta_0}^{\infty}\mathrm{Ai}(\zeta)\,\mathrm{d}\zeta/\mathrm{Ai}'(\zeta_0), \tag{3.64}$$

with functions Gi and Gi′ being defined in Abramowitz & Stegun (1964, p. 449). The exponential decay of H_1 ensures convergence of the integral in (3.61). As will be

shown in §4, P_1 has the asymptote $P_1 = (k^2)$ for $k \ll 1$, implying that P_1 corresponds to an octupole source for sound generation. It consists of two parts: a surface source and volumetric source. That P_1 acts an octupole, as opposed to a quadrupole source, is a consequence of the first kind of source cancellation, namely cancellation in the small-k limit.

It is also found that as $k \to 0$,

$$\tilde{U}_{1,Y} = -\exp(\mathrm{i}\pi/4)\hat{\omega}^{-1/2}\left\{\left[\mathrm{i}\hat{\omega}\tilde{u}_{1,Y}(0)\widehat{F} - \tfrac{1}{2}\int_0^\infty \exp\bigl(-(-\mathrm{i}\hat{\omega})^{1/2}Y\bigr)N_{1,Y}\,\mathrm{d}Y\right]\exp\bigl(-(-\mathrm{i}\hat{\omega})^{1/2}Y\bigr)\right.$$
$$\left. + \tfrac{1}{2}\left[\int_\infty^Y \exp\bigl(-(-\mathrm{i}\hat{\omega})^{1/2}(\tilde{Y}-Y)\bigr)N_{1,\tilde{Y}}\,\mathrm{d}\tilde{Y} - \int_0^Y \exp\bigl(-(-\mathrm{i}\hat{\omega})^{1/2}(Y-\tilde{Y})\bigr)N_{1,\tilde{Y}}\,\mathrm{d}\tilde{Y}\right]\right\} + O(k). \tag{3.65}$$

This indicates that $\tilde{U}_{1,Y}$ and hence $\tilde{U}_1$ are of $O(k^0)$ for $k \ll 1$ with $Y = O(1)$, a result that will be used to decide the radiating nature of certain forcing terms in the subsequent analysis.

Consider now the terms $(\tilde{U}_2,\ \tilde{V}_2,\ \tilde{P}_2)$ in the expansion (3.49). They are governed by

$$\left.\begin{aligned} \mathrm{i}k\tilde{U}_2 + \tilde{V}_{2,Y} &= 0, \\ -\mathscr{L}\tilde{U}_2 + \lambda\tilde{V}_2 &= -\mathrm{i}k\tilde{P}_2 - \tfrac{1}{2}\lambda_2(Y^2\mathrm{i}k\tilde{U}_1 + 2Y\tilde{V}_1) + N_2, \end{aligned}\right\} \tag{3.66}$$

where

$$N_2 = -\bigl\{\mathrm{i}k\tilde{u}_1\tilde{U}_m^{(2)} + \tilde{V}_m^{(2)}\tilde{u}_{1,Y} + \tilde{v}_1\tilde{U}_{m,Y}^{(2)} + \mathrm{i}k\tilde{u}_2\tilde{U}_m^{(1)} + \tilde{V}_m^{(1)}\tilde{u}_{2,Y} + \tilde{v}_2\tilde{U}_{m,Y}^{(1)}\bigr\}. \tag{3.67}$$

Equations in (3.66) can be combined to give

$$\mathscr{L}\tilde{U}_{2,Y} = -N_{2,Y} + \tfrac{1}{2}\lambda_2(Y^2\mathrm{i}k\tilde{U}_{1,Y} + 2\tilde{V}_1). \tag{3.68}$$

As at the leading order, the boundary conditions to be satisfied are

$$\tilde{U}_2 = -\tilde{u}_{2,Y}(0)\widehat{F}, \quad U_{2,YY} = \mathrm{i}\hat{\omega}\tilde{u}_{2,Y}(0)\widehat{F} + \mathrm{i}k\tilde{P}_2 \quad \text{at} \quad Y = 0. \tag{3.69a, b}$$

The right-hand side of (3.68) is proportional to $O(k^0)$ as $k \to 0$. Such a source term in the generic case is expected to be a quadrupole. For the present problem, detailed calculation (below, and in §4) shows this quadrupole contribution from the lower deck turns out to be zero.

Noting that the right-hand side of (3.68) does not decay as $Y \to \infty$, we write

$$\tilde{U}_2 = (\lambda_2/\lambda)\left\{\int_0^Y \tilde{U}_1(Y)\,\mathrm{d}Y - \lambda^{-1}P_1\int_{\zeta_0}^{\zeta} M(\zeta,\zeta_0)\,\mathrm{d}\zeta\right\} + \Pi, \tag{3.70}$$

with $M(\zeta,\zeta_0)$ being defined by (2.38). Then, Π satisfies

$$\mathscr{L}\Pi_Y = -N_{2,Y} + \tfrac{1}{2}(\lambda_2/\lambda)(2N_1 + \mathrm{i}k\lambda Y^2\tilde{U}_{1,Y}) \equiv (\mathrm{i}k\lambda)H_2.$$

On noting that $\tilde{U}_M^{(2)} \sim \lambda_2 A_m^{(1)} Y$ and $\tilde{u}_1^{(2)} \sim \lambda_2 a_1 Y$, the non-decaying part in $N_{2,Y}$ cancels that of N_1 exactly, so that H_2 decays as Y^{-1}. The solution satisfying (3.69a) can be written as

$$\Pi = -\tilde{u}_{2,Y}(0)\widehat{F} + \int_{\zeta_0}^{\zeta}\tilde{M}_2(\zeta,\zeta_0)\,\mathrm{d}\zeta + C_2(k)\int_{\zeta_0}^{\zeta}\mathrm{Ai}(\zeta)\,\mathrm{d}\zeta, \tag{3.71}$$

where $C_2(k)$ is a function of k to be found, and $\tilde{M}_2$ has the same expression as $\tilde{M}_1$ (see (3.58)) except that H_1 is replaced by H_2. On applying the second condition in

(3.69a, b), and matching $\tilde{U}_2$ with its counterpart in the main deck, we obtain

$$\left.\begin{aligned}
&(\mathrm{i}k\lambda)^{2/3}\Big\{\pi\mathrm{Bi}'(\zeta_0)\int_{\infty}^{\zeta_0}\mathrm{Ai}(\zeta)H_2(Y)\,\mathrm{d}\zeta + C_2(k)\mathrm{Ai}'(\zeta_0)\Big\}+\Lambda_0 = \mathrm{i}k\tilde{P}_2,\\
&\int_{\zeta_0}^{\infty}\tilde{M}_2(\zeta)\,\mathrm{d}\zeta + C_2\int_{\zeta_0}^{\infty}\mathrm{Ai}(\zeta)\,\mathrm{d}\zeta + \Lambda_\infty = -\Omega P_1\lambda J_0+\lambda A_2 + \lambda_2 a_1 A_m^{(1)} + \tfrac{3}{2}(\lambda_2/\lambda^2)P_1,
\end{aligned}\right\} \tag{3.72}$$

where

$$\begin{aligned}
\Lambda_0 &= -\mathrm{i}\hat{\omega}\tilde{u}_{2,Y}(0)\widehat{F} + (\lambda_2/\lambda)\Big\{\tilde{U}_{1,Y}(0) - \pi(\mathrm{i}k\lambda)^{2/3}\lambda^{-1}P_1\mathrm{Bi}'(\zeta_0)\int_{\infty}^{\zeta_0}\mathrm{Ai}(\zeta)\,\mathrm{d}\zeta\Big\},\\
\Lambda_\infty &= -\tilde{u}_{2,Y}(0)\widehat{F} - (\lambda_2/\lambda)\Big\{(\mathrm{i}k\lambda)^{-1}\big(\mathrm{i}\hat{\omega}\lambda A_1 - \mathrm{i}kP_1 - \mathrm{i}k\lambda^2 a_1 A_m^{(1)}\big)\\
&\qquad + \lambda^{-1}P_1\Big[\int_{\zeta_0}^{\infty}\Big(M(\zeta,\zeta_0)+\frac{1}{\zeta}\Big)\,\mathrm{d}\zeta - \ln\Omega(\mathrm{i}k\lambda)^{1/3}/(\epsilon\zeta_0)\Big]\Big\}.
\end{aligned} \tag{3.73}$$

After eliminating A_2 and $\tilde{P}_2$ from (3.37) and (3.72), we find that

$$\begin{aligned}
\bar{P}_2 = \frac{-\mathrm{i}(\mathrm{i}k\lambda)^{2/3}\mathrm{Ai}'(\zeta_0)}{k\Delta(k)}\Big\{&\frac{\omega(2-M^2)\lambda}{(1-M^2)^{1/2}|k|k}P_1 + \Omega[J_\infty - J_0 - (1-M^2)I_2]\lambda P_1\\
&+\lambda_2 a_1 A_m^{(1)} - \big(\Lambda_\infty - (\mathrm{i}k\lambda)^{-2/3}\Lambda_0\mathscr{R}(\zeta_0)\big) + \int_{\zeta_0}^{\infty}K(\zeta,\zeta_0)H_2(Y)\,\mathrm{d}\zeta\Big\} - \Omega k^2 I_2 A_1.
\end{aligned} \tag{3.74}$$

The contribution of $\bar{P}_2$ to the acoustic radiation will be comparable to that of P_1 because $\bar{P}_2$ acts as a quadrupole source. Note that $\tilde{U}_{2,Y}$ and $\tilde{U}_2$ are of $O(1)$ for $k \ll 1$ and $Y = O(1)$, as is indicated by the governing equation (3.68) and the solution (3.70).

The terms $(\tilde{U}_3,\ \tilde{V}_3, \tilde{P}_3)$ and R_1 in (3.49) are governed by the equations

$$\left.\begin{aligned}
\mathrm{i}k\tilde{U}_3 + \tilde{V}_{3,Y} &= -\Omega_3 Y\tilde{V}_1 + (\mathrm{i}\hat{\omega} - \mathrm{i}k\lambda Y)\tilde{R}_1 + \tilde{S}_3,\\
-\mathscr{L}\tilde{U}_3 + \lambda\tilde{V}_3 &= -\mathrm{i}k\tilde{P}_3 + \tfrac{1}{2}\Omega_3(Y^2(\mathrm{i}kP_1) - 2Y^2\tilde{U}_{1,YY} - 2Y\tilde{U}_{1,Y})\\
&\quad -\Omega_3\big(\tfrac{1}{6}\lambda Y^3\mathrm{i}k\tilde{U}_1 + \tfrac{1}{2}\lambda Y^2\tilde{V}_1\big) - \tfrac{1}{2}\lambda_2(Y^2\mathrm{i}k\tilde{U}_2 + 2Y\tilde{V}_2)\\
&\quad -\lambda\tilde{R}_{1,Y} + N_3 + \big(\mathrm{i}(k-\alpha)\tilde{\rho}_1 P_m^{(1)} + \mathrm{i}\alpha R_m^{(1)}p_1\big),\\
\mathscr{L}\tilde{R}_1 &= \Omega_3\lambda^{-1}(\lambda Y\tilde{V}_1 + 2\tilde{U}_{1,Y}) + M^2(\mathrm{i}\hat{\omega} - \mathrm{i}k\lambda Y)P_1 + \tilde{E}_3,
\end{aligned}\right\} \tag{3.75}$$

where $\Omega_3 = (\gamma-1)M^2\lambda^2$, N_3 has the same expression as N_2 provided that the sub- and super-scripts '2' are replaced by '3' on the right-hand side of (3.67), and

$$\tilde{S}_3 = -\mathrm{i}k\big(\rho_1\tilde{U}_m^{(1)} + \tilde{u}_1\tilde{R}_m^{(1)}\big) - \big(\rho_1\tilde{V}_m^{(1)} + \tilde{v}_1\tilde{R}_m^{(1)}\big)_Y,$$

$$\tilde{E}_3 = \mathrm{i}(k-\alpha)\tilde{u}_1\tilde{\tau}_m^{(1)} + \tilde{v}_1\tilde{\tau}_{m,Y}^{(1)} + \mathrm{i}\alpha\tilde{\tau}_1\tilde{U}_m^{(1)} + \tilde{V}_m^{(1)}\tilde{\tau}_{1,Y} - (\gamma-1)M^2\big(\mathrm{i}(k-\alpha)\tilde{u}_1 P_m^{(1)} + \mathrm{i}\alpha\tilde{U}_m^{(1)}p_1\big).$$

After eliminating $\tilde{P}_3$ from (3.75), we find

$$\begin{aligned}
\mathscr{L}\tilde{U}_{3,Y} = \Omega_3\big\{&Y(-\mathrm{i}kP_1 + \lambda\tilde{V}_1) + Y^2\tilde{U}_{1,YYY} + 3Y\tilde{U}_{1,YY} + 3\tilde{U}_{1,Y} + \tfrac{1}{6}Y^3(\mathrm{i}k\lambda)\tilde{U}_{1,Y}\big\}\\
&+ M^2\lambda(\mathrm{i}\hat{\omega} - \mathrm{i}k\lambda Y)P_1 + \tfrac{1}{2}\lambda_2(Y^2\mathrm{i}k\tilde{U}_{2,Y} + 2\tilde{V}_2)\\
&- N_{3,Y} + \lambda(\tilde{S}_3 - \tilde{E}_3) - \big(\mathrm{i}(k-\alpha)\tilde{\rho}_{1,Y}P_m^{(1)} + \mathrm{i}\alpha\tilde{R}_{m,Y}^{(1)}p_1\big).
\end{aligned} \tag{3.76}$$

As at the previous order, the forcing term is at most of $O(k^0)$ for $k \ll 1$, and so the contribution from the lower deck is at most a quadrupole, but this is now negligible

compared with the dipole source that must be considered at the present order. Though the full solution for $\tilde{U}_3$ can be obtained using a similar procedure to that for $\tilde{U}_2$, it suffices to write down only the homogeneous part of the solution:

$$\tilde{U}_3 = C_3(k)\int_{\zeta_0}^{\zeta} \mathrm{Ai}(\zeta)\,\mathrm{d}\zeta + \cdots,$$

where C_3 is to be determined by matching with the main-deck solution and applying the boundary condition, which yields

$$\left.\begin{aligned} &C_3(k)\int_{\zeta_0}^{\infty} \mathrm{Ai}(\zeta)\,\mathrm{d}\zeta = (\alpha/k)\big(a_1 P_m^{(1)} - p_1 A_m^{(1)}\big)\lambda I_M + \lambda A_3 + \cdots,\\ &(\mathrm{i}k\lambda)^{2/3} C_3(k)\mathrm{Ai}'(\zeta_0) = \mathrm{i}k\tilde{P}_3 + \cdots. \end{aligned}\right\} \tag{3.77}$$

The solution for $\bar{P}_3$ can be found from (3.44*a*) and (3.77),

$$\bar{P}_3 = \frac{(\mathrm{i}k\lambda)^{2/3}\lambda\mathrm{Ai}'(\zeta_0)}{k^2\Delta(k)}\left\{-\frac{\mathrm{i}\omega\bar{P}_2}{\bar{\kappa}} - \frac{\mathrm{i}\omega^2 P_1}{\bar{\kappa}k}\left[1-\frac{M^2}{2(1-M^2)}\right] - \mathrm{i}\omega A_2 - \mathrm{i}\alpha\big(a_1 P_m^{(1)} - p_1 A_m^{(1)}\big)\lambda I_M\right\}. \tag{3.78}$$

Finally, we consider $(\tilde{U}_4, \tilde{V}_4, \tilde{P}_4)$, which are governed by an inhomogeneous system analogous to (3.75), in which the forcing terms are of $O(k^0)$ at most for small k. Such a quadrupole contribution is negligible compared with the monopole source, so that only the complementary part of the solution is required. It follows from matching with the main-deck solution and the boundary condition that

$$\left.\begin{aligned} &C_4(k)\int_{\zeta_0}^{\infty} \mathrm{Ai}(\zeta) = \lambda A_4 - (\omega\alpha/k^2)\big(a_1 P_m^{(1)} - p_1 A_m^{(1)}\big)\lambda J_M,\\ &(\mathrm{i}k\lambda)^{2/3} C_4(k)\mathrm{Ai}'(\zeta_0) = \mathrm{i}k\tilde{P}_4 + \cdots. \end{aligned}\right\} \tag{3.79}$$

From (3.47)–(3.48) and (3.79), it is found that

$$\begin{aligned}\bar{P}_4 = \frac{(\mathrm{i}k\lambda)^{2/3}\lambda\mathrm{Ai}'(\zeta_0)}{k^2\Delta(k)}\Bigg\{&-\frac{\mathrm{i}\omega}{\bar{\kappa}}\bar{P}_3 - \frac{\mathrm{i}\omega^2\bar{P}_2}{\bar{\kappa}k}\left(1-\frac{M^2}{2(1-M^2)}\right) - \frac{\mathrm{i}\omega^3 P_1}{\bar{\kappa}k^2}\left[1-\frac{M^2(1-2M^2)}{2(1-M^2)^2}\right]\\ &- \mathrm{i}\omega A_3 + F_{4,v} - \frac{\bar{\kappa}}{\mathrm{i}k}F_{4,p} + \mathrm{i}(\omega\alpha/k)\big(a_1 P_m^{(1)} - p_1 A_m^{(1)}\big)\lambda J_M\Bigg\}.\end{aligned} \tag{3.80}$$

4. Acoustic radiation

4.1. *The asymptotic behaviour of the pressure*

The solution for the pressure fluctuation of the scattered field in the upper deck can be written as

$$p_s = \delta h\epsilon\big(p_s^{(1)} + \epsilon p_s^{(2)} + \epsilon^2 p_s^{(3)} + \epsilon^3 p_s^{(4)} + \cdots\big), \tag{4.1}$$

where $p_s^{(j)}$ $(j = 1, 2, 3, 4)$ are the Fourier inversions of $\hat{p}_j$ given by (3.32), (3.35), (3.41) and (3.46). For instance,

$$p_s^{(1)} = \frac{1}{(2\pi)^{1/2}}\int_{-\infty}^{\infty} P_1(k)\exp\big(\mathrm{i}k\bar{x} - (1-M^2)^{1/2}|k|\bar{y}\big)\,\mathrm{d}k. \tag{4.2}$$

In order to calculate the acoustic radiation, it is necessary to know the asymptotic behaviour of p_s as $\bar{x}, \bar{y} \to \infty$. Since the phase of the integrand has no stationary point, the contribution to the integral comes from the region near $k = 0$. Note that as

$k \to 0$, $\zeta_0 \to \infty$. It can be shown that

$$\int_{\zeta_0}^{\infty} \mathrm{Ai}(\zeta)\,\mathrm{d}\zeta/\mathrm{Ai}'(\zeta_0) \sim -\frac{1}{\zeta_0}\big(1-\zeta_0^{-3/2}+O(\zeta_0^{-3})\big), \tag{4.3}$$

$$K(\tilde{\zeta}+\zeta_0,\zeta_0) \sim \frac{1}{\zeta_0}\big(1-\zeta_0^{-3/2}\exp\big(-\zeta_0^{1/2}\tilde{\zeta}\big)-\tilde{\zeta}/\zeta_0+O\big(\zeta_0^{-3}\big)\big), \tag{4.4}$$

for $\tilde{\zeta}=O(\zeta_0^{-1/2})$. Using these results in (3.61) shows that as $k \to 0$,

$$P_1 \sim \mathscr{P}_0 k|k|, \tag{4.5}$$

which implies that $p_s^{(1)}$ corresponds to an octupole with strength $\mathscr{P}_0$,

$$\mathscr{P}_0 = -\frac{\exp(3\pi\mathrm{i}/4)}{\hat{\omega}^{5/2}(1-M^2)^{1/2}}\bigg\{\mathrm{i}\hat{\omega}\tilde{u}_{1,Y}(0)\widehat{F}+\hat{\omega}^{3/2}\exp(-3\pi\mathrm{i}/4)\big(-\lambda a_1 A_m^{(1)}\big) - \mathrm{i}\hat{\omega}^{1/2}\exp(-3\pi\mathrm{i}/4)\int_0^{\infty} Y N_{1,Y}\,\mathrm{d}Y - \int_0^{\infty}\exp\big(-(-\mathrm{i}\hat{\omega})^{1/2}Y\big)N_{1,Y}\,\mathrm{d}Y\bigg\}. \tag{4.6}$$

The formula (4.6) indicates that viscosity determines the strength of the octupole source.

Similarly, it follows from (3.74), (3.78) and (3.80) that

$$\bar{P}_2 \sim -\bigg\{\frac{(2-M^2)\omega}{(1-M^2)}\mathscr{P}_0+\frac{1}{(1-M^2)^{1/2}}\bigg(\frac{\lambda_2}{\lambda}a_1A_m^{(1)}\bigg)\bigg\}|k|, \tag{4.7}$$

$$\bar{P}_3 \sim \bigg\{\frac{(2+M^2)\omega^2}{2(1-M^2)^2}\mathscr{P}_0+\frac{(2-M^2)\omega}{(1-M^2)^{3/2}}\bigg(\frac{\lambda_2}{\lambda}a_1A_m^{(1)}\bigg)\bigg\}\,\mathrm{sgn}(k), \tag{4.8}$$

$$\bar{P}_4 \sim -\bigg\{\frac{M^2(4+M^2)\omega^3}{2(1-M^2)^3}\mathscr{P}_0+\frac{(2+M^2)\omega^2}{2(1-M^2)^{5/2}}\bigg(\frac{\lambda_2}{\lambda}a_1A_m^{(1)}\bigg)\bigg\}|k|^{-1}. \tag{4.9}$$

It can be shown by using Watson's lemma that

$$p_s^{(1)} \sim \frac{-4\mathrm{i}[\bar{x}^3-3(1-M^2)\bar{x}\bar{y}^2]}{[\bar{x}^2+(1-M^2)\bar{y}^2]^3}\mathscr{P}_0, \tag{4.10}$$

$$p_s^{(2)} \sim -\bigg\{\frac{(2-M^2)\omega}{(1-M^2)}\mathscr{P}_0+\frac{1}{(1-M^2)^{1/2}}\bigg(\frac{\lambda_2}{\lambda}a_1A_m^{(1)}\bigg)\bigg\}\frac{2[-\bar{x}^2+(1-M^2)\bar{y}^2]}{[\bar{x}^2+(1-M^2)\bar{y}^2]^2} + 4M^2\omega\mathscr{P}_0\frac{[3\bar{x}^2-(1-M^2)\bar{y}^2]\bar{y}^2}{[\bar{x}^2+(1-M^2)\bar{y}^2]^3}, \tag{4.11}$$

$$p_s^{(3)} \sim \bigg\{\frac{(2+M^2)\omega^2}{2(1-M^2)^2}\mathscr{P}_0+\frac{(2-M^2)\omega}{(1-M^2)^{3/2}}\bigg(\frac{\lambda_2}{\lambda}a_1A_m^{(1)}\bigg)\bigg\}\frac{2\mathrm{i}\bar{x}}{\bar{x}^2+(1-M^2)\bar{y}^2} - \frac{2\mathrm{i}M^4\omega^2\mathscr{P}_0}{1-M^2}\frac{\bar{x}\bar{y}^2[\bar{x}^2-3(1-M^2)\bar{y}^2]}{[\bar{x}^2+(1-M^2)\bar{y}^2]^3} + \bigg\{\frac{M^2(5-2M^2)\omega^2\mathscr{P}_0}{2(1-M^2)} + \frac{M^2\omega}{(1-M^2)^{1/2}}\bigg(\frac{\lambda_2}{\lambda}a_1A_m^{(1)}\bigg)\bigg\}\frac{4\mathrm{i}\bar{x}\bar{y}^2}{[\bar{x}^2+(1-M^2)\bar{y}^2]^2}. \tag{4.12}$$

The relation (4.9) indicates that $\bar{P}_4$ should be understood as a generalized function. The asymptote of $p_s^{(4)}$ is given by (see e.g. Lighthill 1964, p. 43),

$$p_s^{(4)} \sim \left\{ \frac{M^2(4+M^2)\omega^3}{(1-M^2)^3}\mathscr{P}_0 + \frac{(2+M^2)\omega^2}{(1-M^2)^{5/2}}\left(\frac{\lambda_2}{\lambda}a_1 A_m^{(1)}\right)\right\}\left(\ln[\bar{x}^2+(1-M^2)\bar{y}^2]^{1/2}+C\right)$$
$$+\frac{2M^6\omega^3\mathscr{P}_0}{3(1-M^2)}\frac{[3\bar{x}^2-(1-M^2)\bar{y}^2]\bar{y}^4}{[\bar{x}^2+(1-M^2)\bar{y}^2]^3}$$
$$-\left\{\frac{M^4(3-M^2)\omega^3}{(1-M^2)^2}\mathscr{P}_0+\frac{M^4\omega^2}{(1-M^2)^{3/2}}\left(\frac{\lambda_2}{\lambda}a_1A_m^{(1)}\right)\right\}\frac{[-\bar{x}^2+(1-M^2)\bar{y}^2]\bar{y}^2}{[\bar{x}^2+(1-M^2)\bar{y}^2]^2}$$
$$-\left\{\frac{M^2(4+M^2)\omega^3}{(1-M^2)^2}\mathscr{P}_0+\frac{M^2(5-2M^2)\omega^2}{(1-M^2)^{3/2}}\left(\frac{\lambda_2}{\lambda}a_1A_m^{(1)}\right)\right\}\frac{\bar{y}^2}{\bar{x}^2+(1-M^2)\bar{y}^2}, \quad (4.13)$$

where C is an arbitrary constant; its appearance is merely a reflection of the fact that the Laplace equation admits a constant solution (cf. Crow 1970). The far-field asymptotes of $p_s^{(1)}$, $p_s^{(2)}$, $p_s^{(3)}$ and $p_s^{(4)}$ indicate that they act, respectively, as octupole, quadrupole, dipole and monopole sources for the sound radiation.

4.2. *The acoustic field*

The asymptote of the pressure fluctuation in the upper deck implies that the expansion (3.30) ceases to be valid when $\bar{x}=O(\epsilon^{-1})$ and $\bar{y}=O(\epsilon^{-1})$. This suggests the introduction of the variables

$$x^\dagger=\epsilon\bar{x}, \quad y^\dagger=\epsilon\bar{y} \quad (4.14)$$

to describe the acoustic field. Instead of Poisson's equation in the upper deck, the pressure fluctuation now satisfies the convected wave equation in a uniform stream,

$$M^2\left(-\mathrm{i}\omega+\frac{\partial}{\partial x^\dagger}\right)^2 p_s-\left(\frac{\partial^2}{\partial x^{\dagger 2}}+\frac{\partial^2}{\partial y^{\dagger 2}}\right)p_s=0, \quad (4.15)$$

with the boundary condition that $p_s\to 0$ as $r^\dagger\equiv(x^{\dagger 2}+y^{\dagger 2})^{1/2}\to\infty$. The equation is homogeneous since the exponential decay of the T-S wave eigenfunction means that the local forcing vanishes. A solution can be sought of the form

$$p_s=\frac{\delta h\epsilon^4}{\sqrt{2\pi}}p^\dagger(\hat{x},\hat{y})\,\mathrm{e}^{-\mathrm{i}M\hat{x}}, \quad (4.16)$$

where

$$\hat{x}=\frac{M\omega}{1-M^2}x^\dagger, \quad \hat{y}=\frac{M\omega}{(1-M^2)^{1/2}}y^\dagger \quad (4.17)$$

are re-normalized coordinates. In terms of $(\hat{x},\hat{y})$, the governing equation for $p^\dagger$ reduces to the Helmholtz equation

$$\left(\frac{\partial^2}{\partial\hat{x}^2}+\frac{\partial^2}{\partial\hat{y}^2}\right)p^\dagger+p^\dagger=0.$$

The relevant solution for $p^\dagger$ can be expressed as a superposition of multipoles

$$p^\dagger=\left\{s_{11}\frac{\partial^3}{\partial\hat{x}^3}+s_{12}\frac{\partial^3}{\partial\hat{x}^2\partial\hat{y}}+s_{21}\frac{\partial^3}{\partial\hat{x}\partial\hat{y}^2}+s_{22}\frac{\partial^3}{\partial\hat{y}^3}\right.$$
$$\left.+q_{11}\frac{\partial^2}{\partial\hat{x}^2}+q_{12}\frac{\partial^2}{\partial\hat{x}\partial\hat{y}}+q_{22}\frac{\partial^2}{\partial\hat{y}^2}+d_1\frac{\partial}{\partial\hat{x}}+d_2\frac{\partial}{\partial\hat{y}}+m\right\}H_0^{(1)}(\hat{r}), \quad (4.18)$$

where $H_0^{(1)}$ denotes the Hankel function, and $\hat{r}=(\hat{x}^2+\hat{y}^2)^{1/2}$. We may take $s_{12}=s_{21}=0$ and $m=0$ without losing generality because these terms can be expressed as a

combination of the remaining ones in (4.18) by using the identity $H_0^{(1)}(\hat{r}) = -(\partial^2/\partial\hat{x}^2 + \partial^2/\partial\hat{y}^2)H_0^{(1)}(\hat{r})$. The values of the constants s_{11}, s_{22}, q_{11}, q_{12}, q_{22}, d_1 and d_2 can be determined by matching with the upper-deck solution. To that end, we note that for small $\hat{r}$,

$$H_0^{(1)}(\hat{r}) \sim \frac{2\mathrm{i}}{\pi}\left(1-\tfrac{1}{4}\hat{r}^2\right)\ln\hat{r} + \left(1-\tfrac{1}{4}\hat{r}^2\right) + \frac{2\mathrm{i}}{\pi} + \frac{2\mathrm{i}}{\pi}(\ln 2 + \gamma_E - 1)\left(1-\tfrac{1}{4}\hat{r}^2\right) + \cdots, \quad (4.19)$$

with $\gamma_E \approx 0.5772$ being Euler's constant. Inserting (4.19) into (4.18) yields the asymptote of $p^\dagger$ for $\hat{r} \ll 1$. On the other hand, use of (4.10)–(4.13) in (4.1) gives the far-field asymptote of p_s in the upper deck, which is then rewritten in terms of $\hat{x}$ and $\hat{y}$. Matching the two asymptotic expressions, we find that

$$s_{11} = -\frac{\pi M^3\omega^3}{(1-M^2)^3}, \quad s_{22} = 0, \quad (4.20)$$

$$q_{11} = \frac{\pi\mathrm{i}M^2(3+M^2)\omega^3\mathscr{P}_0}{(1-M^2)^3} + \frac{\pi\mathrm{i}(1+M^2)\omega^2}{(1-M^2)^{5/2}}\left(\frac{\lambda_2}{\lambda}a_1A_m^{(1)}\right), \quad (4.21)$$

$$q_{22} = \frac{\pi\mathrm{i}M^2\omega^3\mathscr{P}_0}{(1-M^2)^3} + \frac{\pi\mathrm{i}\omega^2}{(1-M^2)^{5/2}}\left(\frac{\lambda_2}{\lambda}a_1A_m^{(1)}\right), \quad q_{12} = 0, \quad (4.22)$$

and

$$d_1 = \frac{\pi M(1+2M^2)\omega^3\mathscr{P}_0}{(1-M^2)^3} + \frac{2\pi M\omega^2}{(1-M^2)^{5/2}}\left(\frac{\lambda_2}{\lambda}a_1A_m^{(1)}\right), \quad d_2 = 0. \quad (4.23)$$

It is worth mentioning that the matching requirement leads to a massively over-determined system, in which the number of the terms expected to match far exceeds that of the free constants. Nevertheless, it has been verified that once (4.20)–(4.23) are chosen, all the terms match exactly. This, as is usual in the matched asymptotic expansion, serves as a very useful check of our derivation.

The pressure distribution in the acoustic field is therefore described by (4.16) together with (4.18) and (4.20)–(4.23). Of interest is the far-field behaviour of the acoustic pressure. Making use of the fact that $H_0^{(1)}(\hat{r}) \sim \sqrt{2/\pi}\hat{r}^{-1/2}\exp(\mathrm{i}(\hat{r}-\pi/4))$ for large $\hat{r}$, we find that

$$p_s \sim -\frac{(\delta h\epsilon^4)\mathrm{i}}{(1-M^2)^{5/2}}\frac{q(\theta;M,\omega)}{(M\omega r^\dagger)^{1/2}}\exp\left\{\mathrm{i}\left(\frac{M\omega(1-M^2\sin^2\theta)^{1/2}}{1-M^2}r^\dagger - \frac{M^2\omega}{1-M^2}x^\dagger - \frac{\pi}{4}\right)\right\} \quad (4.24)$$

for $\hat{r} \gg 1$, where q is given by

$$q(\theta;M,\omega) = \frac{1}{(1-M^2\sin^2\theta)^{1/4}}\left[1 - \frac{M\cos\theta}{(1-M^2\sin^2\theta)^{1/2}}\right]^2 \times\left\{\omega^3\mathscr{P}_0\left[1 - \frac{\cos\theta/M}{(1-M^2\sin^2\theta)^{1/2}}\right]M^2 + \omega^2(1-M^2)^{1/2}\left(\frac{\lambda_2}{\lambda}a_1A_m^{(1)}\right)\right\}, \quad (4.25)$$

with $\theta \equiv \tan^{-1}(y^\dagger/x^\dagger)$ being the observation angle (see figure 1). It should be pointed out that the above solution is not expected to be valid for $\theta \approx \pi, 0$ because in these two wedged regions at shallow angles to the up/downstream directions, the interchange between the hydrodynamic and acoustic motions is more complicated.

Finally, it may be noted that the scalings (4.14) and (4.17) imply that the motion acquires the acoustic nature at distances $y \sim O(M^{-1}R^{-1/4})$. For $M = 0.2$ and $R = 10^6$,

that amounts to about 160 boundary-layer thickness. Such an estimate provides a guide to the required domain size for direct numerical simulations of sound generation.

5. Variation of the T-S wave amplitude due to scattering

In this section, we calculate the T-S wave downstream of the roughness element. For definitiveness, consider the pressure in the lower deck. In the physical space, the pressure of the scattered field is given by

$$p_s = \frac{\epsilon h \delta}{(2\pi)^{1/2}} \int_{-\infty}^{\infty} \left(P_1(k) + \epsilon \tilde{P}_2(k) + \cdots \right) \mathrm{e}^{\mathrm{i}k\bar{x}} \, \mathrm{d}k. \tag{5.1}$$

It follows from (3.61) and (3.56) that $P_1(k)$ can be split as a sum of two terms, one in which $k = \alpha_1$ is a simple pole, and one in which $k = \alpha_1$ is a branch point, that is

$$P_1 = -\frac{\mathrm{i}(\mathrm{i}k\lambda)^{2/3}\mathrm{Ai}'(\zeta_0)}{k\Delta(k)} \left\{ \tilde{u}_{1,Y}(0)(1 + \zeta_0 \mathscr{R}(\zeta_0)) - \frac{\alpha}{k} \int_{\zeta_0}^{\infty} K(\zeta, \zeta_0) \tilde{u}_{1,Y} \, \mathrm{d}\zeta \right\} \widehat{F}(k - \alpha)$$
$$+ \{\text{the term in which } k = \alpha_1 \text{ is a branch point}\}. \tag{5.2}$$

The branch point contributes only to the near field in the vicinity of the roughness element, while the pole gives rise to the T-S wave, which becomes dominant for $\bar{x} \gg 1$. Somewhat similar to a local receptivity problem (see e.g. Wu 2001), this T-S component appears to have grown from an effective initial amplitude, $\tilde{p}_{s,0}$ say, at $\bar{x} = 0$, and $\tilde{p}_{s,0}$ can be easily evaluated by using the residue theorem. On taking into account the incident T-S wave, the total (equivalent) amplitude of the T-S wave at $\bar{x} = 0$ is $(p_I + \tilde{p}_{s,0})$, that is, the effect of a local roughness element is to 'boost' instantly the amplitude of the T-S wave amplitude to $(p_I + \tilde{p}_{s,0})$. This effect of roughness on the T-S wave can be measured by a *transmission coefficient*, defined as $\mathscr{T}_r = (p_I + \tilde{p}_{s,0})/p_I$. The T-S wave is enhanced by the roughness if $|\mathscr{T}_r| > 1$, and weakened if $|\mathscr{T}_r| < 1$. For simplicity, we consider the Blasius boundary layer only. Then on substituting the result for $\tilde{p}_{s,0}$, it is found that $\mathscr{T}_r$, to leading order, is given by

$$\mathscr{T}_r = 1 + \frac{(2\pi)^{1/2}\mathrm{i}}{\Delta'(\alpha)} \left\{ \tilde{u}_{1,Y}(0)\big(1 + \eta_0 \mathscr{R}(\eta_0)\big) - \int_{\eta_0}^{\infty} K(\eta, \eta_0) \tilde{u}_{1,Y} \, \mathrm{d}\eta \right\} h \widehat{F}(0).$$

Substituting in (2.54) and (3.63) and performing integration by parts in the above expression, we find that the integral term is $(1 + \eta_0 \mathscr{R}) \tilde{u}_{1,Y}(0)$ so that $\mathscr{T}_r = 1$. When the second-order solution (3.74) is used in (5.1), we find that

$$\mathscr{T}_r = 1 + \left\{ \frac{(2\pi)^{1/2}\alpha_2}{\alpha_1 \Delta'(\alpha)} (\mathrm{i}\alpha_1\lambda)^{1/3} \int_{\eta_0}^{\infty} K(\eta, \eta_0)\big(2\eta_0 - \tfrac{4}{3}\eta\big)\mathrm{Ai}'(\eta) \, \mathrm{d}\eta \right\} \epsilon h \widehat{F}(0). \tag{5.3}$$

The above result indicates that roughness shape is irrelevant, and that the gain or reduction in the T-S wave amplitude is proportional to $S \equiv h\widehat{F}(0)$, the (rescaled) area enclosed by the roughness contour.

6. Quantitative results

The physical quantities of interest are the intensity and directivity of the radiated sound (4.25), and also the transmission coefficient (5.3). To evaluate them, it is necessary to compute numerically the base-flow profile and the Airy functions. That is done by a shooting method based on a fourth-order Runge–Kutta method. The various integrals are evaluated using the Trapezoidal rule or Simpson's rule wherever

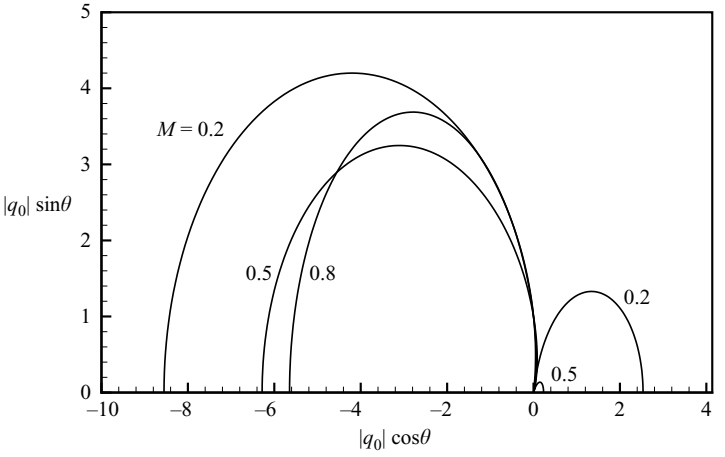

FIGURE 2. The directivity of the acoustic field for the Blasius boundary layer as shown by plotting $q_0(\theta; M)$ (see (6.1)) in the polar coordinate.

possible. For a given frequency ω, the dispersion relation (2.57) is solved by means of Newton iteration to determine the corresponding wavenumber α_1, and the second-order correction, α_2, is calculated using (2.63). In order for the results to be more accessible to a general reader, the familiar non-dimensional frequency, $F = \omega^* \nu_\infty / U_\infty^2 \times 10^6$, will be used in presentation, where ω^* is the dimensional frequency. F is related to ω via

$$F = \omega (T_w / T_\infty)^{-3/2} R^{-3/4} \times 10^6.$$

In all the calculations, we take $R = 10^6$.

6.1. *Acoustic radiation*

In the case of the Blasius boundary layer ($\beta_H = \lambda_2 = 0$), the emitted sound has the same directivity for all frequencies, given by

$$q_0(\theta; M) = \frac{(1 - M^2)^{1/4}}{(1 - M^2 \sin^2\theta)^{1/4}} \left[1 - \frac{\cos\theta / M}{(1 - M^2 \sin^2\theta)^{1/2}}\right] \left[1 - \frac{M \cos\theta}{(1 - M^2 \sin^2\theta)^{1/2}}\right]^2. \quad (6.1)$$

The directivity is illustrated in figure 2 in the form of the usual polar-coordinate plot for three representative Mach numbers. The radiation is characterized by predominantly upstream-propagating acoustic waves. For very low Mach numbers, substantial downstream-propagating sound waves are also generated. However, the downstream radiation diminishes as M increases. The acoustic field exhibits an angle of silence, which is close to the 90° direction for a broad range of $O(1)$ Mach numbers.

While the directivity is independent of the frequency, the intensity of the emitted sound is a strong function of the frequency F. The absolute intensity depends, of course, on the amplitude of the incident T-S wave, as well as on the height and shape of the roughness element. It is useful to normalize the acoustic pressure p_s by writing

$$|p_s| = \epsilon^4 h \delta \widehat{F} a_1 M^{3/2} (1 - M^2)^{-3} \sigma_0 \frac{q_0(\theta)}{\sqrt{r^\dagger}}. \quad (6.2)$$

Then σ_0 is a function of F only, and characterizes the radiating property of T-S waves of different frequencies. The variation of σ_0 with the frequency F is plotted in figure 3 for three representative Mach numbers. In each case, σ_0 increases monotonically with

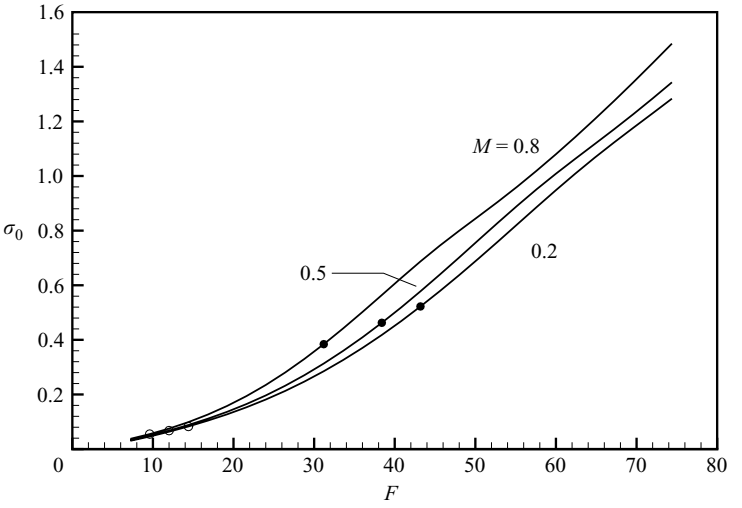

FIGURE 3. Variation of σ_0, defined by (6.2), with the non-dimensional frequency F. ○, The low-branch of the neutral mode; ●, the most unstable mode.

F. This, however, should not be interpreted as implying that a given roughness is most efficient in emitting high-frequency sound waves. The efficiency of a given roughness in radiating sound of different frequencies can be characterized by

$$\sigma_r \equiv \sigma_0 \widehat{F}(-\alpha), \tag{6.3}$$

which may be referred to as a *radiation efficiency coefficient*. As an example, σ_r is calculated for a hump with a Gaussian shape

$$F_w(\bar{x}) = \exp(-\bar{x}^2/\bar{d}^2),$$

where $d \equiv (T_w/T_\infty)^{3/2}\bar{d}$ measures the steepness of the roughness. Figure 4(a) shows σ_r as a function of F for $M = 0.5$ and three values of d. For each d, a salient feature is the appearance of a peak, suggesting that roughness acts as a filter, filtering out components of both very low and high frequencies. The sound emitted by a steep roughness (corresponding to small d) tends to have a broader bandwidth than that by a mild roughness (large d). Figure 4(b) indicates that as the Mach number increases, the peak shifts to high frequencies, and becomes much broader.

The pressure gradient affects radiation in two ways: it modifies the base-flow profile and hence the wall shear λ, and it introduces a quadrupole source corresponding to the second term in (4.25). Its impact is illustrated in the following for the case of $M = 0.2$ and $d = 4$.

When a pressure gradient is present, the directivity of the emitted sound depends on the frequency of the source, and it is no longer possible to write $|p_s|$ as (6.2). Instead, it is written as

$$|p_s| = \epsilon^4 h\delta a_1 M^{3/2}(1 - M^2)^{-3}\frac{q_s(\theta; F)}{\sqrt{r^\dagger}}. \tag{6.4}$$

For a favourable pressure gradient, $\beta_H = 0.2$, the directivity is shown in figure 5(a), where $q_s(\theta; F)$ is plotted against θ for three representative values of F. The radiated sound waves primarily propagate upstream. For comparison purposes, the corresponding result for $\beta_H = 0$ is displayed in the dotted lines. Clearly, the pressure gradient

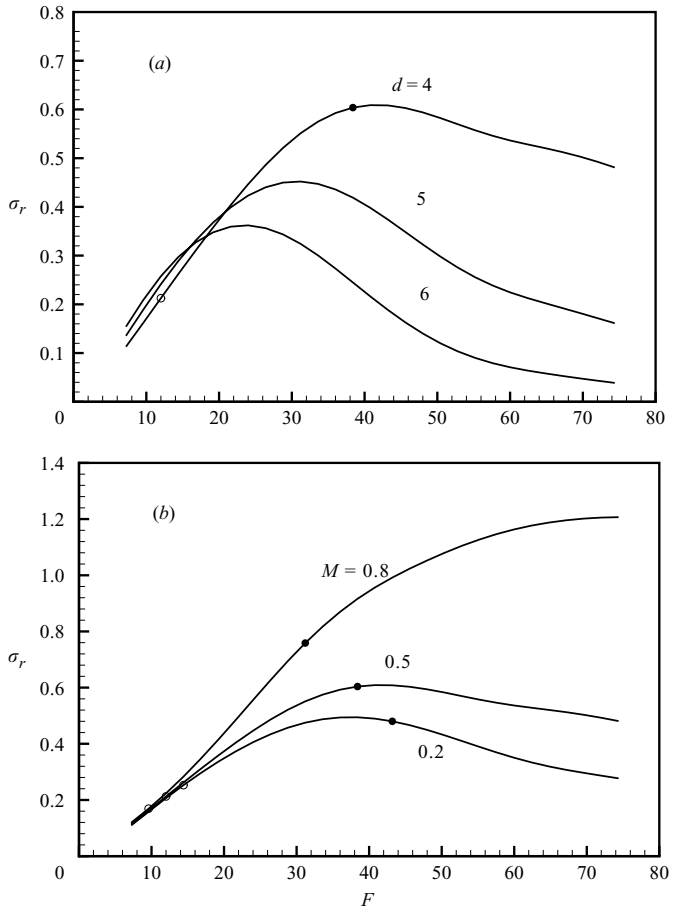

FIGURE 4. Variation of the radiation efficiency function σ_r with F: (a) effect of d ($M = 0.5$); (b) effect of M ($d = 4$). ○, The neutral and ●, the most unstable modes.

has a significant effect at the low-frequency end. Figure 5(b) shows $q_s(\theta; F)$ against the frequency F. A favourable pressure gradient appreciably enhances the efficiency of low-frequency radiation, but moderately reduces that of high-frequency radiation. Although only shown for three directions, the result is typical of all directions. Remember that the present result does not necessarily imply that an accelerating boundary layer is noisier because the absolute sound level depends on the amplitude or spectrum of the instability waves, which in turn depends *inter alia* on receptivity and instability characteristics. Since a favourable pressure stabilizes the boundary layer, T-S waves are likely to be weaker, so that the actual noise level is more likely to be lower.

Figure 6(a) shows the directivity for the case of an adverse pressure gradient corresponding to $\beta_H = -0.08$. Upstream propagating sound waves are predominant, but appreciable downstream emission also occurs. An adverse pressure gradient has a significant impact across the whole frequency range. This is further illustrated in figure 6(b). As opposed to the favourable pressure case, an adverse pressure gradient enhances the efficiency of the high-frequency radiation, while slightly reducing that of the low-frequency radiation.

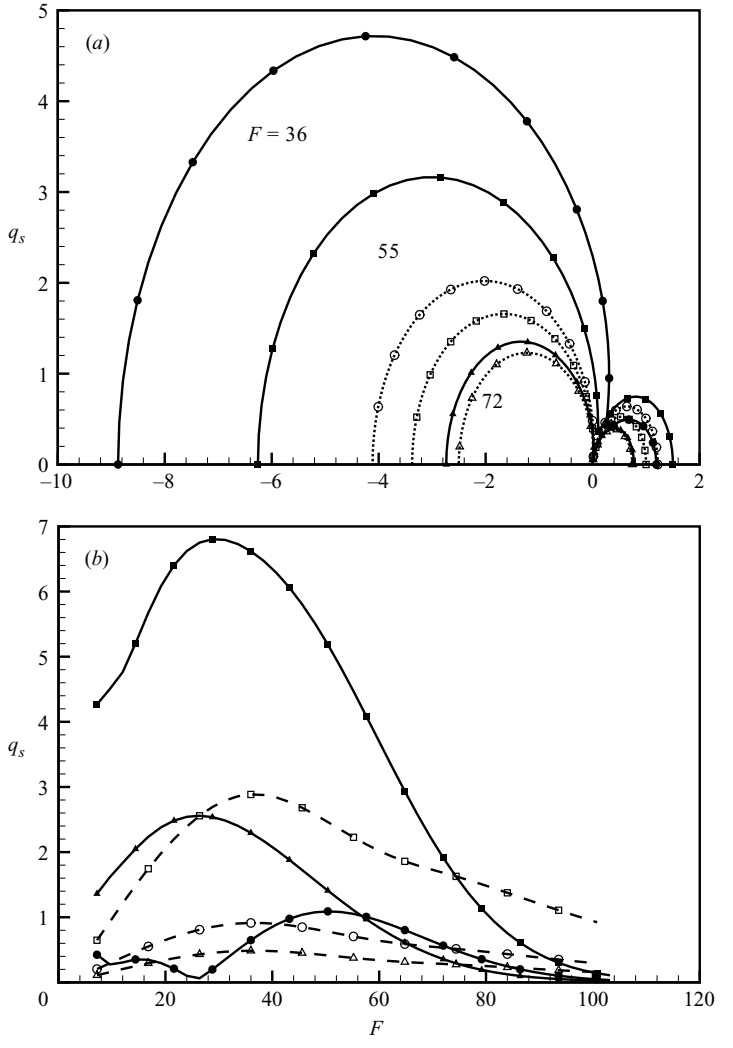

FIGURE 5. (*a*) Directivity of the acoustic field: $q_s(\theta; F)$ in a polar plot for $F = 36$, 55 and 72. (*b*) Radiation efficiency: $q_s(\theta; F)$ *vs.* F along three directions: $\theta = 45°$ (○), 90° (△), and 135° (□). Filled symbols: favourable pressure gradient $\beta_H = 0.2$. Open symbols: $\beta_H = 0$.

6.2. *Transmission coefficient: effect of roughness on the T-S wave*

The transmission coefficient (5.3) is evaluated. A typical result is shown in figure 7. It is found that $|\mathscr{T}_r| > 1$ for $h < 0$, implying that a concave roughness element (i.e. a surface dent) always enhances the T-S wave. For sufficiently small but positive h, $|\mathscr{T}_r| < 1$, suggesting that a surface hump acts as wave barrier to 'block' the T-S wave. Except for the low-frequency band, T-S waves are quite sensitive to roughness. The values of h and d used in figure 7 correspond to a roughness element of just 100 μm in height and 25 mm in width, in a typical laboratory wind-tunnel experiment, with a free-stream speed $U_\infty = 20\,\mathrm{m\,s^{-1}}$. Despite such a mild roughness, (for which the linearized approximation is well justified), the T-S wave amplitude is typically altered by 10 % – 30 %. An effect of this magnitude would be measurable, and it would be interesting to check this prediction experimentally.

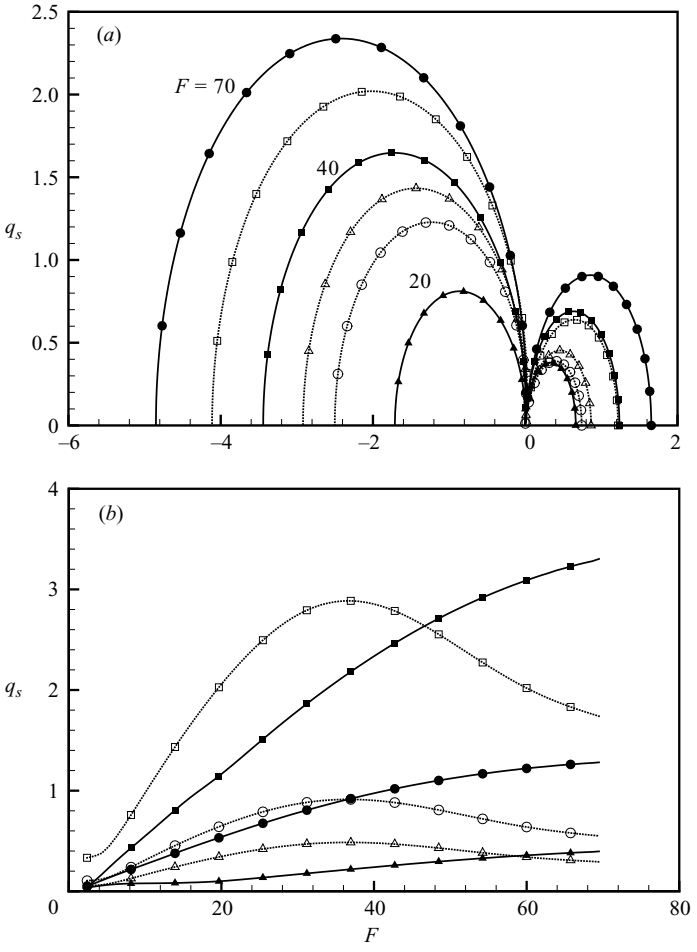

FIGURE 6. (*a*) Directivity of the acoustic field: $q_s(\theta; F)$ in a polar plot for $F = 20$, 40 and 70. (*b*) Radiation efficiency: $q_s(\theta; F)$ *vs.* F along three directions: $\theta = 45°$ (○), 90° (△), and 135° (□). Filled symbols: adverse pressure gradient $\beta_H = -0.08$. Open symbols: $\beta_H = 0$.

That a surface hump may 'stabilize' T-S waves comes as a surprise. However, it should be pointed out that this stabilizing role is restricted to small values of $S = h\widehat{F}(0)$. When S is not small, it is possible that $|\mathscr{T}_r| > 1$. Strictly speaking, a nonlinear calculation is then necessary. Nevertheless, a crude estimate for the critical value of S may be made according to $|\mathscr{T}_r| = 1$. The outcome is displayed in figure 8. The threshold is moderate for the T-S waves with frequencies above that of the locally most unstable mode. If the data is translated to a typical low-speed experiment ($U_\infty = 20\,\mathrm{m\,s^{-1}}$), the threshold for stabilization in the relevant frequency band $40 \leqslant F \leqslant 90$ is found to be in the range of 100–200 μm, beyond which, roughness is expected to have a destabilizing effect, whether it is concave or convex.

It is well known that surface roughness tends to precipitate transition. This has usually been attributed to two distinct mechanisms. The first is receptivity, that is, the roughness-induced mean flow interacts with some free-stream disturbances to generate instability waves. The second is that the roughness distorts the base flow, thereby changing the instability characteristics; this usually happens with extended/distributed

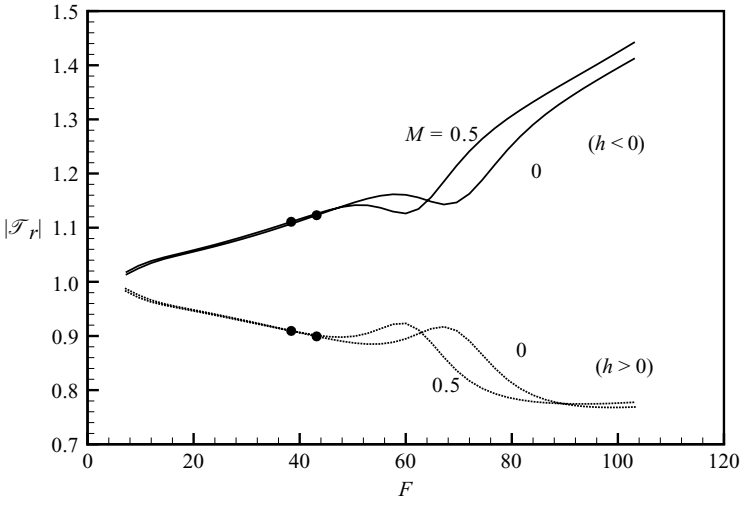

FIGURE 7. Variation of the transmission coefficient $|\mathscr{T}_r|$ with F for Blasius boundary layer. ●, Most unstable modes. Solid lines, $h < 0$. Dashed lines, $h > 0$.

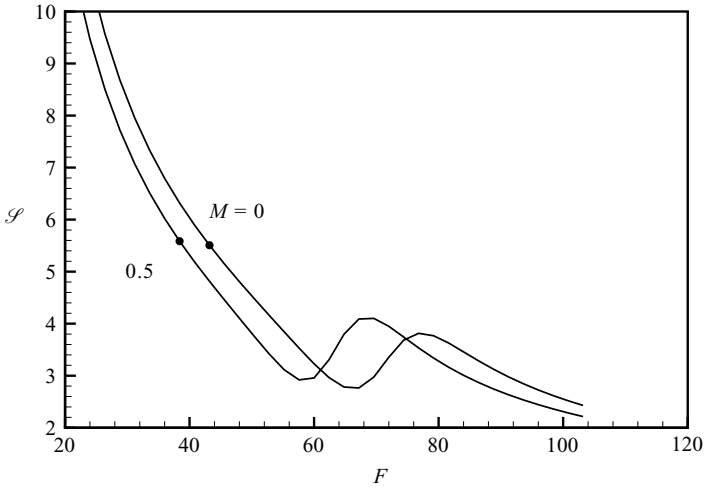

FIGURE 8. The estimated threshold value of $\mathscr{S}$ below which a surface hump has a stabilizing effect. ●, Most unstable modes.

surface roughness, or large isolated roughness height which may produce a region of separated flow. The present scattering by a localized roughness element represents yet another mechanism, which is different in that roughness affects the propagation of pre-existing T-S waves.

7. Summary and concluding remarks

In this paper, an asymptotic approach based on triple-deck theory was extended to analyse the acoustic radiation of a T-S wave as it is scattered by a local roughness. It is found that the acoustic field consists of predominately upstream propagating sound waves. The mean pressure gradient affects the radiation significantly and in a subtle way (i.e. by generating a quadrupole source in the main part of boundary layer).

From the methodology point of view, the present asymptotic approach, which treats the source as an integral part of sound generation, has a certain advantage over the acoustic analogy approach. The hydrodynamic motion is analysed in detail. The radiating property of various source terms is decided by examining, in the Fourier space, the small-wavenumber limit of the solutions forced by them. This allows for a systematic and unambiguous identification of relevant sources. A correct prediction of the radiated sound requires knowledge of both the strength of the hydrodynamic sources and their radiating property, characterized by the asymptotic and multipole orderings, respectively. Weaker lower-order multipolar sources can be just as important as stronger higher-order sources.

A fundamental feature of aerodynamic sound generation is cancellation among sources, which leads to a tiny fraction of energy being radiated to the far field as acoustic waves. This accordingly is also a cause of difficulty for accurate prediction. The cancellation in the present problem was revealed in some detail. The first type of cancellation occurs in the spectral space in the small-k limit, as a result of which the largest forcing term (from the lower deck) acts as an octupole, rather than a quadrupole as one might expect. A similar cancellation leading to reduced radiation takes place in the upper deck. The second type of cancellation is in physical space, e.g. between the dipole sources from the main and upper decks.

In the present approach, viscosity appears at leading-order in the lower deck, and moreover directly controls the strength of the octupole source, thereby affecting the overall intensity (and also the directivity if $\beta_H \neq 0$) of the emitted sound. In contrast, the wave operator in any acoustic analogy theory ignores viscosity completely. An interesting question is: how could the latter be used to solve the present problem? Given that the sound wave is generated by the mutual interaction between the T-S wave and the mean-flow distortion, one might propose to calculate the sound emission using (3.26), the 'source term' in which may be evaluated beforehand using, for example, the O-S solutions for both the mean-flow distortion and the T-S wave. However, this seemingly reasonable procedure would not yield the correct answer because it neglects viscosity, which has been shown to be controlling sound emission. It appears, therefore, that the viscous-scattering problem will have to be solved beforehand, and the resulting solution will be used to model the relevant source.

Acoustic radiation of instability waves undergoing rapid distortion is suggested as an important physical mechanism for generating noise in subsonic flows. The problem considered in this paper represents a relatively simple situation. As mentioned in § 1, rapid distortion occurs when instability waves interact with a sharp corner or a trailing edge. The basic asymptotic framework is currently being extended to investigate those sound-generation problems, which are closely related to air-frame noise.

The present study also indicates that a minimal local surface roughness has a significant effect on the amplitude of the T-S wave, and hence on the transition as a whole.

X.W. is indebted to late Professor W. C. Reynolds for the encouragement in the early stage of the present work, which was started in 2001 while X.W. was visiting Stanford University. The authors benefited from the stimulating discussions with Dr Meelan Choudhari during his visit to Imperial College London, which was sponsored by an EPSRC visiting fellowship (GR/S59635). Thanks also go to Professor M. Gaster for the discussion relating to the impact of local roughness on T-S waves, to Professors J. T. Stuart and H. Zhou for helpful comments, and to the referees for

various suggestions, which helped improve the manuscript. L. H. was supported by an EPSRC studentship (GRP00772/01).

Appendix. Definitions of integrals and forcing terms

$$I_2 = \int_0^\infty \left(R_B U_B^2 - 1\right) \mathrm{d}y, \tag{A 1}$$

$$I_M = \gamma M^2 - \int_0^\infty \left[(\gamma - 1)M^2\left(\frac{R_B'}{R_B} - \frac{U_B'}{U_B}\right) + \frac{R_B'}{R_B^2 U_B^2}\right] \mathrm{d}\tilde{y}, \tag{A 2}$$

$$J_0 = aM^2 - \int_0^a \left(\frac{1}{R_B U_B^2} - \frac{T_w}{T_\infty}\frac{1}{\lambda^2 y^2}\right) \mathrm{d}y + \frac{T_w}{T_\infty}\frac{1}{\lambda^2 a}, \tag{A 3}$$

$$J_\infty = \int_a^\infty \left(\frac{1}{R_B U_B^2} - 1\right) \mathrm{d}y - (1 - M^2)a, \tag{A 4}$$

$$J_M = \int_0^\infty \left\{(\gamma - 1)M^2\left(\frac{R_B'}{R_B U_B} - \frac{U_B'}{U_B^2}\right) + \frac{2R_B'}{R_B^2 U_B^3}\right\} \mathrm{d}\tilde{y} + \tfrac{1}{2}(\lambda_2/\lambda)(\gamma - 1)M^2\Omega^{-1}. \tag{A 5}$$

In the above expressions, the parameter a is arbitrarily provided, $a \neq 0$.

The forcing terms in (3.13) are:

$$S_3 = -\mathrm{i}k\left(u_1 R_m^{(2)} + \rho_1 U_m^{(2)} + u_2 R_m^{(1)} + \rho_2 U_m^{(1)}\right) - \left(v_1 R_m^{(2)} + \rho_1 V_m^{(2)} + v_2 R_m^{(1)} + \rho_2 V_m^{(1)}\right)_{\tilde{y}}, \tag{A 6}$$

$$\begin{aligned} D_3 = {} & -R_B\left(\mathrm{i}k u_1 U_m^{(2)} + v_1 U_{m,\tilde{y}}^{(2)} + u_{1,\tilde{y}} V_m^{(2)}\right) - R_B\left(\mathrm{i}k u_2 U_m^{(1)} + v_2 U_{m,\tilde{y}}^{(1)} + u_{2,\tilde{y}} V_m^{(1)}\right) \\ & + \Omega\left(\mathrm{i}\alpha p_1 R_m^{(1)} + \mathrm{i}(k - \alpha)\rho_1 P_m^{(1)}\right)/R_B, \end{aligned} \tag{A 7}$$

$$\begin{aligned} E_3 = {} & \mathrm{i}\omega R_B\left(\tau_1 R_m^{(1)} + \rho_1 \tau_m^{(1)}\right) - \mathrm{i}k R_B U_B\left[\tau_1 R_m^{(2)} + \tau_m^{(1)}\rho_2 + \rho_1 \tau_m^{(2)} + R_m^{(1)}\tau_2\right] \\ & + (\gamma - 1)M^2\Omega\left\{U_B\left(\mathrm{i}\alpha p_1 R_m^{(1)} + \mathrm{i}(k - \alpha)P_m^{(1)}\rho_1\right) - R_B\left(\mathrm{i}\alpha p_1 U_m^{(1)} + \mathrm{i}(k - \alpha)u_1 P_m^{(1)}\right)\right\} \\ & + R_B^2\left[\mathrm{i}\alpha\tau_1 U_m^{(2)} + \mathrm{i}(k - \alpha)u_1\tau_m^{(2)} + V_m^{(2)}\tau_{1,\tilde{y}} + v_1\tau_{m,\tilde{y}}^{(2)}\right] \\ & + R_B^2\left[\mathrm{i}\alpha\tau_2 U_m^{(1)} + \mathrm{i}(k - \alpha)u_2\tau_m^{(1)} + V_m^{(1)}\tau_{2,\tilde{y}} + v_2\tau_{m,\tilde{y}}^{(1)}\right], \end{aligned} \tag{A 8}$$

$$\begin{aligned} G_3 = {} & -R_B\left(\mathrm{i}\alpha v_1 U_m^{(1)} + \mathrm{i}\alpha(k - \alpha)u_1 V_m^{(1)} + v_1 V_{m,\tilde{y}}^{(1)} + V_m^{(1)} v_{1,\tilde{y}}\right) \\ & + \Omega^{-1}\left(R_m^{(1)} p_{2,\tilde{y}} + \rho_1 P_{m,\tilde{y}}^{(2)}\right)/R_B. \end{aligned} \tag{A 9}$$

The forcing terms in (3.45) are:

$$\begin{aligned} R_{4,p} = {} & \left\{-(1 - M^2)^{3/2}(\alpha_1 + \mu)[(1 - M^2)\alpha_2 + M^2\omega]\left(1 - \frac{\mu}{k - \alpha}\right)(k - 2\alpha)\bar{y}\right. \\ & + (1 - M^2)[(1 - M^2)\alpha_2 + M^2\omega]\left(1 - \frac{\mu}{k - \alpha}\right)(k - 2\alpha) \\ & + (1 - M^2)(\alpha_1 + \mu)\left[-(q - (k - 2\alpha)\omega/\alpha_1)\left(1 - \frac{\mu}{k - \alpha}\right) + \alpha_2\right] \\ & - (1 - M^2)\left(1 - \frac{\mu}{k - \alpha}\right)\alpha\alpha_2 - M^2 q\left[\frac{\gamma M^2 + 1}{(1 - M^2)^{1/2}} - \frac{(1 - M^2)^{1/2}\mu}{k - \alpha}\right]\bar{y}k^2 \\ & \left. + M^2\left[-2\gamma q + (k - 2\alpha)(\omega/\alpha_1)\left(1 - \frac{\mu}{k - \alpha}\right) - \frac{2q\mu}{k - \alpha}\right]k\right\} p_1 P_m^{(1)}, \end{aligned} \tag{A 10}$$

$$R_{4,v} = \left\{(1-M^2)[(1-M^2)\alpha_2 + M^2\omega]\left(1-\frac{\mu}{k-\alpha}\right)(k-2\alpha)\bar{y} + (1-M^2)^{1/2}\left[(q-(k-2\alpha)\omega/\alpha_1)\left(1-\frac{\mu}{k-\alpha}\right)-\alpha_2\right]\right\} p_1 P_m^{(1)}. \quad \text{(A 11)}$$

REFERENCES

Abramowitz, M. & Stegun, I. A. 1964 *Handbook of Mathematical Functions*. National Bureau of Standards.

Akylas, T. R. & Toplosky, N. 1985 The sound field of a Tollmien–Schlichting wave. *Phys. Fluids* **29**, 685–689.

Arbey, H. & Bataille, J. 1983 Noise generated by airfoil profiles placed in a uniform laminar flow. *J. Fluid Mech.* **134**, 33–47.

Bechert, D. & Pfizenmaier, E. 1975 On the amplification of broadband jet noise by pure tone excitation. *J. Sound Vib.* **43**, 581–587.

Bishop, K. A., Ffowcs Williams, J. E. & Smith, W. 1971 On the noise sources of the unsuppressed high-speed jet. *J. Fluid Mech.* **50**, 21–31.

Bridges, J. & Hussain, F. 1992 Direct evaluation of aeroacoustic theory in a jet. *J. Fluid Mech.* **240**, 469–501.

Cargill, A. M. 1982 Low frequency sound radiation and generation due to the interaction of unsteady flows with a jet pipe. *J. Fluid Mech.* **121**, 59–105.

Crighton, D. G. & Huerre, P. 1990 Shear-layer pressure fluctuations and superdirective acoustic source. *J. Fluid Mech.* **220**, 355–368.

Crow, S. C. 1970 Aerodynamic sound emission as a singular perturbation problem. *Stud. Appl. Maths* **49**, 21–44.

Crow, S. C. 1972 Acoustic gain of a turbulent jet. *Am. Phys. Soc. Meeting, Univ. Colorado, Boulder*, paper IE.6.

Crow, S. C. & Champagne, F. H. 1971 Orderly structure in jet turbulence. *J. Fluid Mech.* **48**, 547–591.

Ffowcs Williams, J. E. & Kempton, A. J. 1978 The noise from the large-scale structure of jet. *J. Fluid Mech.* **84**, 673–694.

Goldstein, M. E. 1984 Sound generation and upstream influence due to instability wave interacting with non-uniform mean-flows. *J. Fluid Mech.* **149**, 161–177.

Goldstein, M. E. 1985 Scattering of acoustic waves into Tollmien–Schlichting waves by small streamwise variations in surface geometry. *J. Fluid Mech.* **154**, 509–529.

Haj-Hariri, H. & Akylas, T. R. 1986 Sound radiation by instability wavepackets in a boundary layer. *Stud. Appl. Maths* **75**, 57–76.

Ho, C.-M. & Huang, L.-S. 1982 Subharmonics and vortex merging in mixing layer. *J. Fluid Mech.* **119**, 443–473.

Howe, M. S. 1975 Contributions to the theory of aerodynamics sound, with application to excess jet noise and the theory of the flute. *J. Fluid Mech.* **71**, 625–673.

Howe, M. S. 1976 The influence of vortex shedding on the generation of sound by convected turbulence. *J. Fluid Mech.* **76**, 711–740.

Howe, M. S. 1978 A review of theory of trailing edge noise. *J. Sound Vib.* **61**, 437–465.

Huerre, P. & Crighton, D. G. 1983 Sound generation by instability waves in a low Mach number jet. *AIAA Paper* 83-0661.

Kambe, T. 1986 Acoustic emissions by vortex motions. *J. Fluid Mech.* **173**, 643–666.

Kibens, V. 1980 Discrete noise spectrum generated by an acoustically excited jet. *AIAA J.* **18**, 434–441.

Laufer, J. & Yen, T.-C. 1983 Noise generation by a low-Mach-number jet. *J. Fluid Mech.* **134**, 1–31.

Lighthill, M. J. 1952 On sound generated aerodynamically. *Proc. R. Soc. Lond.* A **211**, 564–587.

Lighthill, M. J. 1964 *An Introduction of Fourier Analysis and Generalized Functions*. Cambridge University Press.

Lilley, G. M. 1974 On the noise from jets, noise mechanisms. *AGARD-CP* 131, pp. 13.1–13.12.

McLaughlin, D. K., Morrison, G. L. & Troutt, T. R. 1975 Experiments on the instability waves in a supersonic jet. *J. Fluid Mech.* **69**, 73–95.

Mitchell, B. E., Lele, S. K. & Moin, P. 1999 Direct computation of the sound generated by vortex pairing in an axisymmetric jet. *J. Fluid Mech.* **383**, 113–142.

Moore, C. J. 1977 The role of shear-layer instability waves in jet exhaust noise. *J. Fluid Mech.* **80**, 321–367.

Munt, R. M. 1977 The interaction of sound with subsonic jet issuing from semi-infinite cylindrical pipe. *J. Fluid Mech.* **83**, 609–640.

Nash, E. C. & Lowson, M. V. 1999 Boundary-layer instability noise on airfoils. *J. Fluid Mech.* **382**, 27–61.

Obermeier, F. 1967 Berechnung aerodynamisch erzeugter Schallfelder mittels der Mthode der 'Matched Asymptotic Expansions'. *Acustica* **18**, 238–240.

Phillips, O. M. 1960 On the generation of sound by supersonic turbulent shear layers. *J. Fluid Mech.* **9**, 1–27.

Smith, F. T. 1973 Laminar flow over a small hump on flat plate. *J. Fluid Mech.* **57**, 803–824.

Smith, F. T. 1979 On the nonparallel flow stability of the Blasius boundary layer. *Proc. R. Soc. Lond.* A **366**, 91–109.

Smith, F. T. 1989 On the first-mode instability in subsonic, supersonic or hypersonic boundary layers. *J. Fluid Mech.* **198**, 127–153.

Stewartson, K. 1974 Multistructured boundary layers on flat plates and related bodies. *Adv. Appl. Mech.* **14**, 145–239.

Tam, C. K. W. 1971 Directional acoustic radiation from a supersonic jet generated by shear layer instability. *J. Fluid Mech.* **46**, 757–768.

Tam, C. K. W. 1972 On the noise of a nearly ideally expanded supersonic jet. *J. Fluid Mech.* **51**, 69–95.

Tam, C. K. W. 1995 Supersonic jet noise. *Annu. Rev. Fluid Mech.* **27**, 17–43.

Tam, C. K. W. & Burton, D. E. 1984*a* Sound generated by instability waves of supersonic flow. Part 1. Two dimensional mixing layers. *J. Fluid Mech.* **138**, 249–271.

Tam, C. K. W. & Burton, D. E. 1984*b* Sound generated by instability waves of supersonic flow. Part 2. Axisymmetric jets. *J. Fluid Mech.* **138**, 273–295.

Tam, C. K. W. & Morris, P. J. 1980 The radiation of sound by the instability waves of a compressible plane turbulent shear layer. *J. Fluid Mech.* **98**, 349–381.

Troutt, T. R. & McLaughlin, D. K. 1982 Experiments on the flow and acoustic properties of a moderate-Reynolds-number supersonic jet. *J. Fluid Mech.* **116**, 123–156.

Wang, M., Lele, S. K. & Moin, P. 1996 Sound radiation during laminar breakdown in a low-Mach-number boundary layer. *J. Fluid Mech.* **319**, 197–218.

Wu, X. 2001 On local boundary-layer receptivity to vortical disturbances in the free stream. *J. Fluid Mech.* **449**, 373–393.

Wu, X. 2002 Generation of sound and instability waves due to unsteady suction and injection. *J. Fluid Mech.* **453**, 289–313.

Wu, X. 2005 Mach wave radiation of nonlinearly evolving supersonic instability modes in shear flows. *J. Fluid Mech.* **523**, 121–159.

Zaman, K. B. M. Q. 1985 Far-field noise of a subharmonic jet under controlled excitation. *J. Fluid Mech.* **152**, 83–111.